UC Davis
San Francisco Estuary and Watershed Science

Title

Investigation of Floating Peat Wetlands, Sacramento—San Joaquin Delta, California

Permalink

https://escholarship.org/uc/item/43w4j002

Journal

San Francisco Estuary and Watershed Science, 22(4)

Authors

Deverel, Steven

Jeffres, Carson

Dore, Sabina

et al.

Publication Date

2024

DOI

10.15447/sfews.2024v22iss4art2

Supplemental Material

https://escholarship.org/uc/item/43w4j002#supplemental

Copyright Information

Peer reviewed

RESEARCH

Investigation of Floating Peat Wetlands, Sacramento–San Joaquin Delta, California, USA

Steven Deverel[*1], Carson Jeffres[2], Sabina Dore[1], Nicholas Corline[2], Nicholas Christen[1], Liyi Xu[1], Marc Olds[1], Savannah M. Haas[1], Gregory G. Shellenbarger[3], Daniel Eckes[1]

DATA ACCESSIBILITY STATEMENT

Explanatory detail and data for Appendices A through D are available at the following Figshare link: *https://figshare.com/articles/dataset/Floating_Peat_Supplementary_Data/24775476*

ABSTRACT

Tidal wetland restoration is integral to achieving the Delta coequal goals. Deeply subsided islands limit the potential for tidal wetland restoration. Floating peats may offer an opportunity to create tidal habitat in the subsided western and central Delta. We conducted a mesocosm experiment to assess the feasibility of floating peat blocks, and the potential food-web benefits, biomass production, carbon sequestration, methane emissions, and water-quality effects. We evaluated the effect of varying water residence time and initial peat-block density.

The peat blocks floated during the entire experiment, and accreted biomass at rates consistent with those reported for Delta non-tidal managed wetlands. Peat blocks placed in mesocosms with 45% open water expanded horizontally about 21% per year. We estimated average vertical accretion rates of 5.5 to 8.6 cm yr^{-1} for all the mesocosms. Vertical and horizontal expansion increase floating peat-block stability.

We measured a 3-fold zooplankton population increase during the first year after deployment, relative to the Mokelumne River, which was the mesocosm's water source. Measured and modeled methane emissions were lower than those reported in Delta non-tidal managed wetlands. Aqueous methane concentrations and methane fluxes were significantly lower for the shorter water-residence-time of about 5 days compared to longer residence times of about 11 days. Elevated dissolved oxygen (DO) concentrations generally corresponded with low methane concentrations. Our estimated net ecosystem carbon balance of – 820 +/– 137 g C m^{-2} yr^{-1} indicates that the floating wetlands are potentially greater carbon sinks than Delta non-tidal wetlands. Nitrogen data indicated consumption by wetland plants, and denitrification and dissimilatory nitrate reduction in the mesocosms. Our preliminary results point to potential ecosystem benefits of floating peats on a larger scale.

KEY WORDS

INTRODUCTION AND BACKGROUND

The Delta Reform Act established two coequal goals: securing a reliable water supply for California and protecting, restoring, and enhancing the Sacramento–San Joaquin Delta ecosystem and the fish, wildlife, and recreation it supports. Restoring tidal wetlands is central to achieving these coequal goals. Draining Delta islands for agriculture in the 19th and 20th centuries resulted in a 98% decrease in the area of tidal marsh (Cloern et al. 2021), and subsidence, which caused land surface elevations to decrease to well below sea level (Deverel, Ingrum, et al. 2016a). Draining tidal wetlands depleted soil carbon stocks by oxidizing soil organic matter (Windham–Myers et al. 2023), which currently releases an estimated 1.2 million metric tons of CO_2-equivalents into the atmosphere annually (Vaughn et al. 2024). Oxidation of soil organic matter is the primary cause of subsidence and represents a significant source of California agricultural greenhouse gas (GHG) emissions.

Hydrologic interventions to reduce Delta GHG emissions include impounded non-tidal marshes to reverse subsidence, agricultural management practices, and tidal re-introduction and connectivity (Windham–Myers et al. 2023). Flooding the soil reduces the GHG emissions that result from the oxidation of the organic soils (Hemes et al. 2019). Over decades, permanently flooded, managed wetlands provide a net GHG emissions reduction benefit relative to the oxidizing organic soils, and reverse the effects of subsidence, thereby reducing levee vulnerability (Arias–Ortiz et al. 2021; Deverel et al. 2020; Hemes et al. 2019; Deverel, Bachand, et al. 2016b; Deverel et al. 2014; Miller et al. 2008).

Restoration of tidal wetlands will benefit species of concern and support pelagic habitat. However, subsidence limits the potential to restore tidal wetlands on Delta islands. Accretion within the permanently flooded Twitchell West Pond wetland created in 1997 ranged from 470 to 594 mm during 1998–2018 (Deverel et al. 2020). Deverel et al. (2014) estimated that over 100 years will be required for managed non-tidal wetlands to reach intertidal range elevations on most of the subsided central and western Delta. Sea level rise and levee failure may reduce or eliminate the potential for these wetlands to accrete to intertidal range elevations. Tidal wetland restoration on subsided islands will be limited by the cost and availability of the large volumes of fill material required to bring elevations to within tidal ranges. For example, to restore tidal marsh on Franks Tract, the California Department of Fish and Wildlife (2020) estimated that over 28,000,000 cubic meters of fill material would be required. For comparison, Northwest Hydraulic Consultants (2006) estimated a total annual availability of Delta dredge spoil of about 450,000 cubic meters. Flooded, deeply subsided islands will likely not provide significant benefits for native species as evidenced by Franks Tract and Mildred Island, which are home to few native species and high proportions of alien species (Durand 2017). Floating peat wetlands on or adjacent to subsided islands potentially offer an opportunity for tidally connected marsh habitat.

Background

Floating Peat Wetlands

Floating peat wetlands have been studied worldwide: in the Gulf Coast marshes of Louisiana and the Mississippi River Delta (Russell 1942; Hatton et al. 1983; Sasser and Gosselink 1984; Sasser et al. 1996; Swarenski et al. 2005; Izdepski et al. 2009); in Florida (Mallison et al. 2001); in the Netherlands (Lamers et al. 1999; Tomassen et al. 2004); and in Russia (Volkova 2010). Swarzenski et al. (1991) reported the occurrence of floating peats in the Sudd on the Nile River, East Africa; floodplain lakes of the Middle Amazon; the Romanian Danube Delta region, and the Okavango Delta. Floating peat islands in the pre-development Sacramento–San Joaquin Delta were reportedly as large as several acres, and over 3 m thick (Whipple et al. 2012). A livestock herd remained safe on a floating peat island near Venice Island during the 1862 flood (Whipple et al. 2012).

In his study of Delta Quaternary climatic records, which included organic soils and remnant plant materials, Atwater (1980) stated that *Scirpus acutus* (now *Schoenoplectus acutus*) was the most frequent species. Dachnowski–Stokes (1933) (as reported by Atwater 1980) regarded much of the peat as detritus of hypothetical floating mats and recognized macroscopic fragments of both "tule" (*Schoenoplectus acutus*) and "reed" (*Phragmites australis*) in peat soils beneath farmed islands. Delta floating islands described in Whipple et al. (2012) were likely formed from such peats. We were unable to find descriptions of floating *Schoenoplectus acutus* peats in other locations. Mallison et al. (2001) reported long-term floatation of *Schoenoplectus cubana*.

Floating peats have very low dry bulk density (Swarzenski et al. 1991; Holm et al. 2000; Smolders et al. 2002; Tomassen et al. 2004) and organic matter contents that range from 47% to 91% (Swarzenski et al. 1991; Sasser et al. 1996), and they contain extensive root systems. Reported dry bulk densities for floating peats in the southeastern US ranged from 0.029 to 0.16 g cm^{-3} (Swarzenski et al. 1991; Sasser et al. 1996). *Typha* floating mat roots in Louisiana extended to about 30 cm below the surface (van Donselaar-ten Bokkel Huinink 1961). Lamers et al. (1999) and Tomassen et al. (2004) reported that floating peat organic matter generates methane, which contributes to flotation.

The Delta Ecosystem

Before the 1850s, the Sacramento–San Joaquin Delta was a complex of aquatic habitats which included tidal marshes that provided nutrient cycling, carbon sequestration, and fisheries habitat (Opperman et al. 2009; Cloern et al. 2021). Whipple et al. (2012) mapped the extent of freshwater emergent tidal wetlands, which included the area of present-day subsided organic (peat) soils (Deverel, Bachand, et al. 2016b). These peat soils formed under anaerobic conditions during the last 6,000 years (Drexler et al. 2009; Whipple et al. 2012). Organic deposition kept pace with sea level rise (Mount and Twiss 2005). Food webs in these landscapes sustained high rates of primary productivity, fueled by a combination of biologically available organic matter produced by native marsh and floodplain vegetation, and phytoplankton produced in the channels and open waters (Brown et al. 2016). After the 1850s, floodplain and Delta wetland habitats were reduced by 95% (Whipple et al. 2012). Ecosystem net primary productivity was reduced by 94%, carbon (energy) flow to herbivores by 89%, and detritus production by 94% (Cloern et al. 2021). Invasive species also reduced primary production (Jassby et al. 2003). Native fish abundances significantly declined for species that used the Delta as rearing habitat and migratory species (Moyle and Leidy 1992).

In the pre-development Delta, tidal marshes linked to open waters produced biologically available organic matter and primary producers (phytoplankton and microalgae) (Robinson et al. 2016); and provided habitat and food for fish (Jassby and Cloern 2000; Brown et al. 2016). Archaea and bacteria mediated biogeochemical processes (Mosier and Francis 2008), which contributed energy to higher trophic levels, often through a zooplankton trophic transfer (Ederington et al. 1995). Howe et al. (2014) reported that Delta emergent tidal marsh vegetation produced biologically active organic matter, which was transformed into food energy for invertebrates that, in turn, became fish prey. On Liberty Island, Whitley and Bollens (2014) concluded that restored tidal marsh provided abundant food and prey resources, including zooplankton. The endangered Delta Smelt feeds primarily on zooplankton (Moyle et al. 1992; Lott 1998; Moyle 2002; Nobriga 2002; Hobbs et al. 2006).

Increasing Delta water temperatures may limit native fish habitation by inducing physiological stress or by decreasing DO levels. Projected higher water temperatures may render waters near the confluence of the Sacramento and San Joaquin rivers, historically inhabited by Delta Smelt, largely uninhabitable by this species (Brown et al. 2013). Wagner et al. (2011) projected an increased number of days with elevated temperature that can cause fish mortality (especially along the Sacramento River) and a shift to earlier spawning. Delta Smelt showed physiological sensitivity to

increased temperature compared to control fish (Davis et al. 2019). Under warming conditions, Delta Smelt, when fed to satiation, are likely able to maintain the energy allocation required for body maintenance and growth (Davis et al. 2019). If food resources are low, the physiological adjustments required to maintain homeostasis under warming may be energy limited.

Hypotheses and Approach

Literature review and data analysis led to the hypothesis that recently accreted Twitchell West Pond sediments, where *Schoenoplectus acutus* and *Typha* species dominated (Miller and Fujii 2010), would float. In 2018, HydroFocus personnel removed the aboveground biomass, excavated a block of about 0.3 m³ of accreted wetland sediment, and witnessed floatation. The excavated wetland block remained floating, and surface vegetation and roots grew. Larger peat blocks were subsequently excavated and floated in a small pool.

We hypothesized that floating peat wetlands could provide ecosystem services in the subsided Delta, and conducted a mesocosm experiment in which we attempted to address the following questions.

- What are the potential food-web and fish-habitat benefits?

- What are the nature and effects of biomass accumulation and accretion?

- What are the GHG emissions—and removals, and the processes, and factors that affect these?

- What are the water-quality effects and related processes?

We used large mesocosms as a first step to assess processes that affect floating peats in a controlled environment. Treatments were intended to understand variations in invertebrate populations, water quality, and GHG fluxes and processes that affect these variations. Mesocosms have been successfully used to study wetland processes (Ahn and Mitsch 2002; Salimi et al. 2021). Limitations include the inability to simulate the complex array of interactions in natural ecosystems (Ahn and Mitsch 2002). The size of our mesocosms allowed many of the ecosystem processes that could be affected by residence time and initial floating peat coverage to be simulated with two replicates.

Project Location and Mesocosms

On Bouldin Island in 2019, we constructed eight aboveground mesocosms (Doughboy swimming pools) about 5.5 m in diameter and about 1.2 m deep, plus associated water delivery and drainage infrastructure (Figure 1). We excavated peat blocks from the Twitchell Island West Pond wetland created in 1997 (Miller et al. 2008) and placed them in the mesocosms, which received water via siphon from the adjacent Mokelumne River (Figure 1). We excavated approximately 280 m² of peat blocks with biological oversight (to ensure protection of threatened animal species) and under the US Army Corps of Engineers Nationwide Permit 40. Aboveground vegetation was removed before the peat blocks were transported to Bouldin Island.

We established two treatments to evaluate varying residence time (long residence time or LRT of 10.9 days, and short residence time or SRT of 5.16 days) and initial low-density coverage (45%) and high-density coverage (93%) of floating peat blocks (open and closed), in two replicates each (Appendix A, Figure A1). We utilized inflow and outflow meters to regulate and calculate mesocosm residence time. We selected residence times based on discussions with Dr. Peter Moyle of the University of California– Davis Center for Watershed Science. Blocks placed in the mesocosms in July 2019 (Figure 2) were fully vegetated by September 2019, and there was substantial wetland biomass growth in June 2020 (Figure 3). All blocks remained floating during the entire study, which extended from July 2019 until January 2022, and continue floating as of this writing. The blocks also grew together to form larger floating masses, and willow trees have grown on the floating peat wetlands.
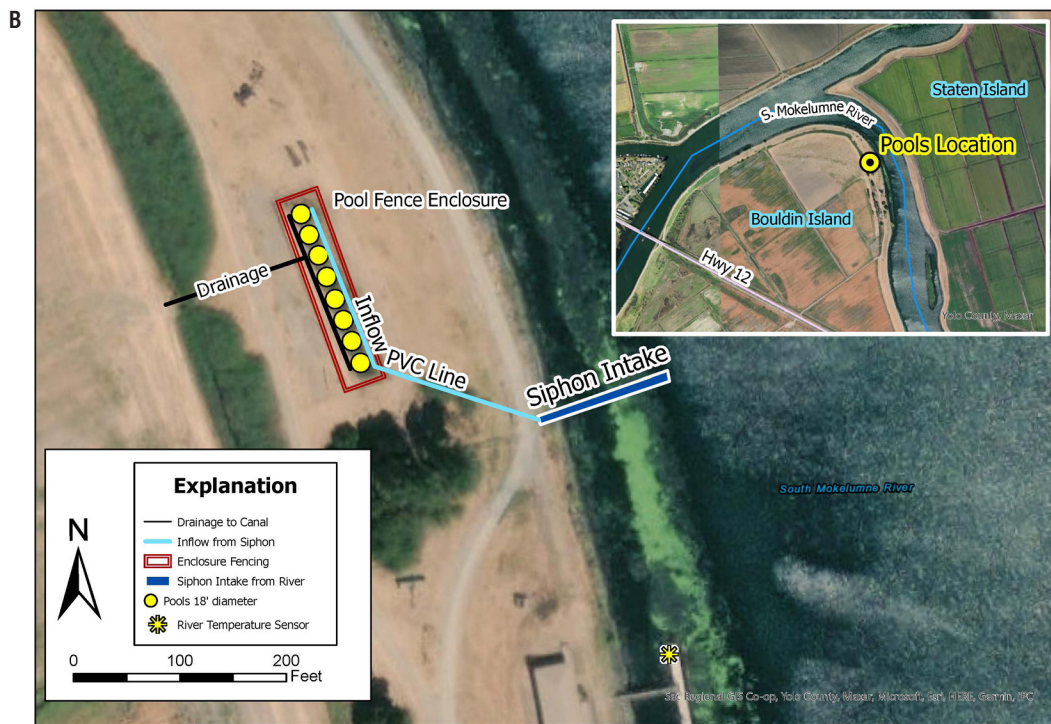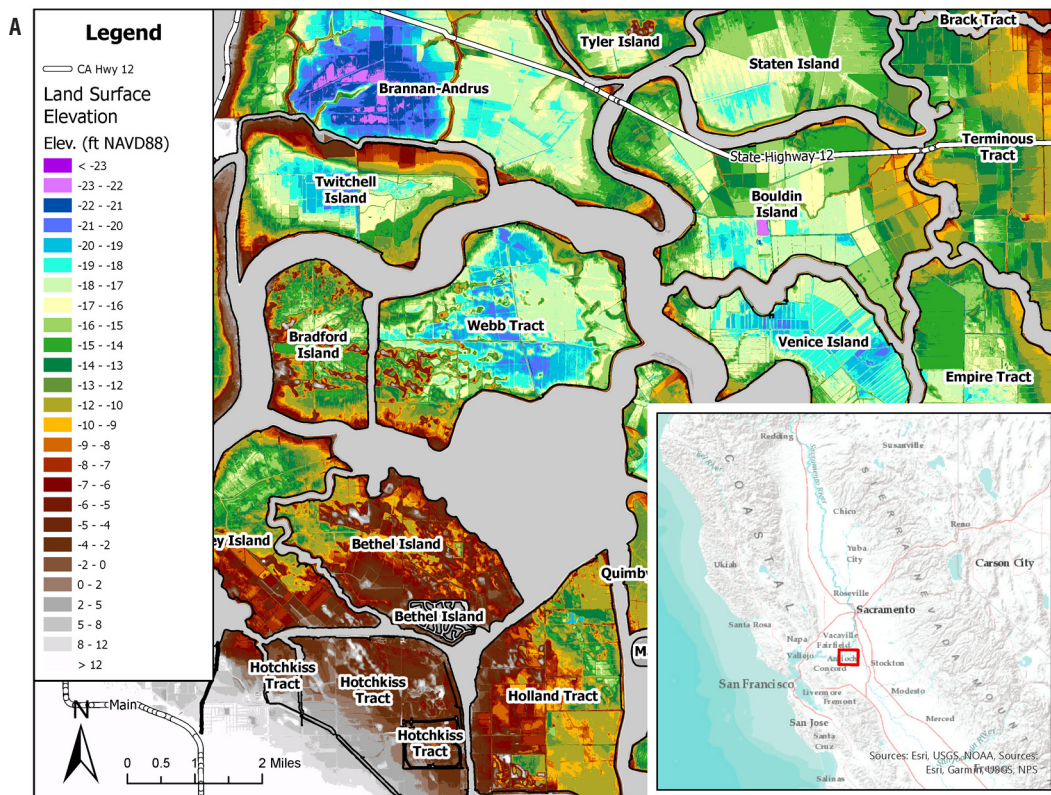
Figure 1 (**A**) Location of Bouldin Island (owned by Metropolitan Water District) and land surface elevations, (**B**) pool location and water lines adjacent to the Mokelumne River

METHODS

Flow Measurements and Residence Time Calculations

We installed McCrometer Ultra Mag electromagnetic flow meters (model UM06, *https://www.mccrometer.com/ultra-mag/ product?id=52003823655)* to measure flows in and out of the mesocosms and to maintain specified residence times. We averaged the inflow and outflow rates for each mesocosm pair to determine the flow rate through a mesocosm pair (Appendix A, Figure A1). Table 1 shows flow rates and residence times for the four different mesocosm treatments, and Appendix A describes calculations and data analysis.

Figure 2   Placement of peat blocks in mesocosms in July 2019

Figure 3   Wetland vegetation on floating peats in June 2020, about 11 months after placement

Table 1 Flow rates and residence times for treatments

Treatment	Average flow rate (L minute⁻¹)	Average residence time and standard error in parentheses (days)
Short residence time (SRT): mesocosms 1 and 3	22.1	5.16 (0.28)
Long residence time (LRT): mesocosms 2 and 4	2.83	10.9 (0.04)
Low-density peat block coverage (Open): mesocosms 6 and 8	4.01	7.62 (0.025)
High-density peat block coverage (Closed): mesocosms 5 and 7	4.47	6.58 (0.021)

Food Web and Fish Habitation

Zooplankton and Macroinvertebrates

We collected zooplankton and macroinvertebrate samples from August 2019 to June 2020. However, in early March 2020, field and laboratory operations at UC–Davis were suspended as a result of COVID-19 remote-work and shelter-in-place orders. We were unable to collect the April 2020 zooplankton samples and resumed sampling in June 2020. We sampled zooplankton by vertical tows, by lowering a 30-cm-diameter, 150-µm-mesh zooplankton net 1 m into each mesocosm and then pulling it to the surface. We then rinsed net contents into sample containers. We repeated this process three times for a total volume of 0.21 m³ sampled per mesocosm. We also collected zooplankton samples in the Mokelumne River adjacent to the mesocosm pools (N 38.129407, W -121.563057). The Mokelumne River was a "seed source" and represented the ambient invertebrate and zooplankton community in the area of the study. Following the protocols of Corline et al. (2017), we threw a zooplankton net 5 m out from the levee interface with the Mokelumne River and retrieved it four times for a total sample volume of 1.4 m³. To account for the Mokelumne River's changing flow conditions, we attached a flow meter to the zooplankton net and recorded starting and ending flows. Each sample was placed into a Whirl-Pak® and preserved in 95% ethanol with Rose Bengal dye.

We rinsed zooplankton samples through a 150-µm-mesh filter into a beaker with a known quantity of water; volumes varied depending on sample zooplankton density. We then sub-sampled these samples using a 1-mL large-bore pipette. Using a dissecting scope with 4-10x magnification, we enumerated zooplankton until at least one hundred individuals of the most frequent taxonomic group, and one hundred individuals of all other taxonomic groups combined, were counted. If these two conditions were not met, we counted every individual in the sample. We used the volume of the sample in the beaker and the sub-sampled volume to estimate the density of zooplankton in each sample. We standardized sample results to total volume sampled to compare among treatments and the Mokelumne River. We identified zooplankton using keys from Thorp and Covich (2009) and Hanley (2020).

We sampled for macroinvertebrates by dragging a 500-µm-mesh kick net along the bottom of each mesocosm for 10 seconds and then scraping the net against the bottom of a floating peat block for an additional 10 seconds. The contents in the kick net were then elutriated, placed in Whirl-Paks® and preserved in 95% ethanol with Rose Bengal dye. We rinsed samples through a colander to remove large detritus, and we filtered the rinsed portion through a 150-µm-mesh net. Elutriation is a process for separating particles based on their size, shape, and density. We did this in the field to separate organic material and invertebrates from mineral sediments via swirling the sample and pouring off the lighter non-mineral material. We examined macroinvertebrate samples using a dissecting scope at 4x to 10x magnification. We examined each sample twice to ensure we collected all macroinvertebrates. For all samples, we identified macroinvertebrates to the lowest possible taxonomic group and enumerated using keys from Merritt et al. (2008) and Thorp and Covich (2009).

Temperature

In the mesocosms at depths of 15 cm and 110 cm, and in the Mokelumne River at a depth of 110 cm, we collected hourly water-temperature

data using *in situ* data loggers (HOBO TidbiT v2 Temp Logger, Onset Computer Corporation). We placed temperature sensors in the mesocosm north and south ends, farthest away from inlets and outlets. Using the Mann–Whitney test, we analyzed the differences between Mokelumne River and mesocosm temperatures during June, July, and August. The Mann–Whitney rank–sum test determines whether one group contains significantly different observations than a second group (Helsel and Hirsch 2002). We used the R-Stat program (Version 4.1.3, R Core Team 2022) Mann–Whitney test to determine if there were significant differences at a 95% confidence level. We made no assumptions about how data were distributed in either group.

Biomass and Accretion

Biomass
Before placement in the mesocosms in July 2019, we collected one sample from each of three blocks in each mesocosm using a wetland coring device (Hargis and Twilley 1994). We analyzed peat block samples for bulk density and organic matter content using methods described in Blake and Hartge (1986) and Nelson and Sommers (1996). In August 2020 and October 2021, we collected biomass samples and measured the leaf-area index (LAI). We collected biomass samples within 20-cm x 40-cm areas in each mesocosm and determined wet and dry weights. To collect the belowground biomass samples in the floating peat blocks, we used a saw to create a hole with a diameter of 7.95 cm and extracted the biomass and measured the depth of the sample core in the peat block. We determined total carbon in above- and below-surface biomass samples using methods described in Nelson and Sommers (1996) at the UC–Davis Analytical Laboratory and DellaValle Laboratory in Fresno, California.

We measured the LAI (see Appendix B for a descriptions of methods), which is defined as the one-sided green leaf area per unit ground surface area (Dronova and Taddeo 2016) in 2020 and 2021. We assessed the relationship of the LAI and the camera Normalized Difference Vegetation Index (NDVI). Using a drone and camera with an

infra-red filter (Survey3, MAPIR, Inc., San Diego, California), we conducted biweekly to monthly flights to determine NDVI. The camera NDVI provides a measure of vegetation greenness by calculating the difference between near-infrared light that is reflected by plants, and red light that is absorbed by plants.

$$NDVI = \frac{NIR - Red}{Red + NIR} \qquad \textbf{Eq 1}$$

where NIR = spectral reflectance measurements in the near-infrared spectrum, Red = spectral reflectance measurements in the red spectrum.

We used NDVI to estimate LAI, which was used to calculate wetland gross primary production (GPP). Using drone imagery, we determined the percent of the mesocosm area that was occupied by peat blocks and open water. Appendix B contains details about drone imagery and NDVI calculations.

Accretion
We did not find documented methods for measuring short-term (annual) accretion in floating peats. Folse et al. (2020) and Bianchette et al. (2015) excluded accretion measurements for floating marshes. Long-term accretion (decadal) has been measured using lead and cesium isotopes (e.g., Nyman et al. 2006). We estimated accretion using the results of biomass sampling and bulk density measurements, modeling, and measurements of peat block thickness. In July 2019, we measured the dimensions of peat blocks before we placed them in the mesocosms. In September 2021, the water in the mesocosms was drawn down temporarily, and we measured the thickness of the peat blocks in all mesocosms by measuring the distance from the top of the peat blocks to the top of the mesocosms. We estimated the accretion rate as the difference between the 2021 and 2019 peat-block thickness measurements.

Methane and Carbon Dioxide Fluxes
To measure methane and carbon dioxide fluxes (fCH$_4$ and fCO$_2$), we placed dark chambers on collars inserted in the peat blocks. To fabricate

chambers, we used non-CH_4-emitting material, impermeable, and non-reactive low-density polyethylene (LDPE, PVC, and rubber). Adhesive and caulk used for the collar and chamber components did not provide a source of CH_4 during laboratory testing. We constructed two identical cylindrical static chambers as per Pavelka et al. (2018) using low-density opaque polyethylene sheeting. We fully extended the cylindrical chamber over the vegetation. To prevent deformity of the flexible wall material, chamber wall design included rigid PVC rings that had the same diameter and wall thickness as the 12-inch PVC collars. We calculated total chamber volume of 121 L using a diameter of 31.2 cm and height of 158 cm. We accounted for additional volume from the height of the collar above the peat-block surface, generally about 1 to 2 cm, during flux calculations. A small fan powered by a 9-volt battery located at the chamber top provided circulation. We sampled chamber air from an outlet connected to a 6-mm-outside-diameter intake tube that extended the height of the chamber with perforations every 7 cm to facilitate collection of vertically integrated samples.

We vented chambers to equilibrate with atmospheric pressure and reduce pressure effects during chamber placement. We designed and constructed our vents based on Hutchinson and Livingston (2001), who estimated that chamber CO_2 loss through a vent tube with an inside diameter of 9 mm and a length of 15 cm was less than 0.04% of the total flux for a 14-L chamber over a 30-minute measurement period. We placed vent tubes in the chamber side walls with a downward-facing outlet to minimize wind perturbations (Hutchinson and Livingston 2001). To test for leaks, we sealed the chambers on galvanized metal sheeting, filled the chamber with N_2 gas, and measured changes in chamber CH_4 concentrations over time as per Pavelka et al. (2018). We applied wind stress across chamber surfaces using a fan. Our leak test for both chambers averaged 0.001 µmol CH_4 m^{-2} s^{-1}, less than 1.1% of the average of fCH_4 field measurements in the floating peat mesocosms during 2020–2022.

We inserted beveled PVC collars for chamber placement 10 to 15 cm below peat-block surfaces, which was consistently below the water level. The required insertion depth for achieving a seal under such waterlogged soil conditions is a few mm, because the water-filled pore spaces effectively provide a barrier to gas transport (Matson and Harris 2009). We measured and recorded CH_4 and CO_2 concentrations vs. time with a self-calibrating Li-COR Li-7810 trace gas analyzer using Optical Feedback–Cavity-Enhanced Absorption Spectroscopy (OF-CEAS). We hung the chamber enclosure on a cable system positioned above the floating peat blocks at the correct height for connecting to the collars, encompassing the vegetation, and maintaining a constant chamber volume. Before measurement, we opened the chamber lid to allow equilibration of CH_4 and CO_2 concentrations inside the chamber with ambient concentrations. The chamber fan was switched on, and the chamber was then placed carefully over the wetland vegetation and onto the collar. Clamps at the chamber–collar interface ensured that the weather-stripping junction was airtight. The linear portion of the concentration vs. time plot, which typically lasted for about 2 minutes, provided the basis for flux calculations (Livingston and Hutchinson 1995). We measured flux consistently (during mid-morning) in all eight mesocosms. We multiplied the slope of the CH_4 and CO_2 increases with time by the enclosure volume and divided by the chamber basal area to obtain fCH_4 and fCO_2 values, as outlined in Parkin and Venterea (2010).

Simulation of Greenhouse Gas Emissions and Removals

We employed the Peatland Ecosystem Photosynthesis Respiration and Methane Transport-Dual Arrhenius Michaelis–Menton (PEPRMT–DAMM) model (Oikawa et al. 2017) to (1) simulate processes in the mesocosm labile carbon and soil organic carbon pools, (2) integrate the collected data and provide insights about processes that affect GHG fluxes, (3) estimate the net ecosystem exchange, and (4) estimate accretion. The model was originally developed for Delta permanently flooded non-tidal wetlands and parametrized using eddy covariance data for the Twitchell Island West Pond and Sherman

Island Mayberry wetlands. Heretofore, it has not been used to simulate processes in floating peats. Inputs included air temperature, plant photosynthetic active radiation (PAR), water table height (WT), and data for soil organic carbon (SOC) and labile carbon pools. The model calculates ecosystem respiration (Reco), gross primary productivity (GPP), methanogenesis, hydrodynamic fluxes and plant-mediated transport of CH_4 and CO_2, and net ecosystem exchanges of CH_4 and CO_2.

Carbon is added to the system through plant photosynthesis, and manifests as GPP, which is released via ecosystem respiration. Photosynthetic active radiation (PAR) and LAI were used to calculate GPP using a light use efficiency (LUE) model (Gamon 2015; Knox et al. 2017):

$$GPP = \varepsilon * \text{fAPAR} * \text{PAR} * f(T) \qquad \textbf{Eq 2}$$

where ε is LUE and $f(T)$ is a temperature function. Photosynthesis increases exponentially with temperature until the optimum temperature is reached, above which photosynthesis is inhibited. The PEPRMT model was used to calculate fAPAR using the LAI estimated from NDVI data (Ruimy et al. 1999):

$$\text{fAPAR} = 0.95 * (1 - e^{-k*LAI}) \qquad \textbf{Eq 3}$$

where fAPAR is the fraction of the solar radiation absorbed for photosynthesis, and k is the extinction coefficient which we assumed to be 0.8, based on Oikawa et al. (2017). We assumed that all GPP entered the labile carbon pool and was available for decomposition.

The model simulated fCO_2 ($fCO2_{model}$) from Reco based on the Dual Arrhenius Michaelis–Menten (DAMM) kinetics model and is a function of temperature, labile C, SOC, and WT (Equation 4). Reco outputs the substate availability of the two C pools:

$$Reco = \left(\frac{V_{max_{SOC}} \times [C_{SOC_{avail}}]}{k_{M_{SOC}} + [C_{SOC_{avail}}]} + \frac{V_{max_{labile}} \times [C_{labile}]}{k_{M_{labile}} + [C_{labile}]} \right) \times f(WT)_{Reco} \qquad \textbf{Eq 4,}$$

$$V_{max\,x} = \alpha_x * e^{-Ea_x/RT} \qquad \textbf{Eq 5,}$$

$$[C_{SOC_{avail}}] = [C_{SOC_{total}}] \times k_{soc} \qquad \textbf{Eq 6,}$$

where V_{max} is the maximum rate of respiration enzyme kinetics for the respective C pools when substrate concentrations are not limiting. V_{max} is calculated from the Arrhenius function (Equation 5), where α_x is the base rate of CO_2 production for each C substrate, Ea_x is each substate's activation energy for CO_2 production, R is the universal gas constant, and T is the air temperature. The fraction of available SOC ($C_{SOC_{avail}}$) is determined by K_{SOC} (Equation 6), which is 0.5 if the wetland is less than 3 years old, or 0.2 if older, to account for elevated respiration after wetlands are restored (Oikawa et al. 2017). The $k_{M_{SOC}}$ and $k_{M_{labile}}$ are the half-saturation respiration concentrations for each C substrate. The water table correction function ($f(WT)_{Reco}$) accounts for anaerobic conditions that inhibit respiration.

The model simulated fCH_4 ($fCH4_{model}$) using the DAMM equation (Equation 7) paired with temperature sensitivity using the V_{max} calculated from the Arrhenius function (Equation 5) (Davidson et al. 2012; Davidson et al. 2014; Oikawa et al. 2017; Sihi et al. 2019).

$$fCH4_{model} = \left(\frac{V_{max_{SOC}} * [C_{SOC\,avail}]}{kM_{SOC} + [C_{SOC\,avail}]} + \frac{V_{max_{labile}} * [C_{labile}]}{kM_{labile} + [C_{labile}]} \right) * f(WT) * f(WT)_{wetland\,age} \qquad \textbf{Eq 7}$$

where C_{labile} is the available carbon in the labile C pool, and $C_{SOC_{avail}}$ is the available C in the SOC pool, and kM_{SOC} and kM_{labile} are the Michaelis–Menten constants for the respective substrates. $f(WT)$ is the WT height correction function, which accounts for O_2 inhibition of CH_4 if the water table falls below the wetland surface. The V_{max} in Equation 7 is the maximum rate of methanogenesis for the respective C pools when substrate concentrations are not limiting (Oikawa et al. 2017), and was calculated using Equation 5, where α_x is the base rate of CH_4 production for each substrate and Ea_x is the activation energy for CH_4 production.

In the model, CH_4 is released to the atmosphere via ebullition, plant vascular tissue, and diffusion. The mesocosm WT height was specified as 5 cm above the peat block surface, as per field observations. The model also accounts for the inhibitory effect of water salinity and sulfate concentrations on CH_4 emissions (Oikawa et al. 2017). We used atmospheric input data for the PEPRMT model from the nearby California Irrigation Management Information System (CIMIS) station and on-site measurements. We used LAI and LUE to calculate GPP. We used the annual average salinity and sulfate concentrations determined during water-quality sampling and analysis for the eight mesocosms as model inputs. For this study, the initial SOC fraction was the average of the data for the peat blocks, and the labile C pool was estimated from mesocosm biomass samples. We initially assumed that model inputs for the floating peat mesocosms were the same as for the Twitchell West Pond wetland (Oikawa et al. 2017).

We optimized model parameters using a limited-memory modification of the quasi-Newtonian method from Byrd et al. (1995), which allowed for optimization with specified upper and lower constraints on targeted parameters. To match measured fCH_4 and fCO_2, we identified a set of target parameters and provided initial values from the Twitchell Wetland model to be varied to optimize output. Limited memory approximation of the Hessian matrix that contains second-order partial derivatives for the changes in model outputs provided parameter matrices that were used for model sensitivity analysis. We adjusted model inputs—which included LUE and temperature sensitivity to CH_4 production, activation energy, Ea_x (from the Michaelis–Menten Equation 5) for the SOC and labile carbon pools—to simulate measured fCH_4 and fCO_2 during January 2020 to January 2022. Appendix C (see "Data Accessibility Statement" for link) describes our model inputs for optimization and provides a comparison with the Oikawa et al. (2017) Twitchell West Pond wetland model.

Water Quality

From July 2019 to January 2022, we collected water samples that we analyzed using methods described in Appendix D (see "Data Accessibility Statement"). Water quality constituents included major ions (calcium, magnesium, sodium, potassium, chloride, sulfate, bicarbonate), total dissolved solids, dissolved organic carbon (DOC), CH_4, total organic carbon (TOC), nitrate (NO_3-N), and ammonia. We collected water samples, and water-quality parameters (pH, specific conductance, and DO) were measured following standard methods provided in Appendix D. We used the Mann–Whitney test to compare concentrations and parameter values among treatments.

RESULTS

Food Web and Fish Habitation

During 1 year after deployment, zooplankton and macroinvertebrate sampling results demonstrated the ability of the floating peats to support these populations at levels greater than the Mokelumne River in the pelagic space between the benthos and the peat mat. The zooplankton community consisted of small bodied cladocerans (water fleas) and cyclopoid and calanoid copepods. Cladoceran species were primarily *Alona* species, *Chydorus sphearicus*, and unidentified chydorids; cyclopoid and calananoid copepods were largely composed of *Acanthocyclops* species and *Psuedodiaptomus* species. There were large temporal variations in abundance and between mesocosms (Figure 4). Overall, the average zooplankton population density in the samples collected from the mesocosms was over 300% greater than the adjacent Mokelumne River samples (Figure 5).

Macroinvertebrate populations were variable both temporally and within treatments (Figure 6). The first sampling effort resulted in few invertebrates, while the last three samples indicated increased colonization. The non-native snail *Cipangopaludina chinensis* was the most numeric taxa, followed by the dipteran family Chironomidae and the amphipod *Gammarus* species.
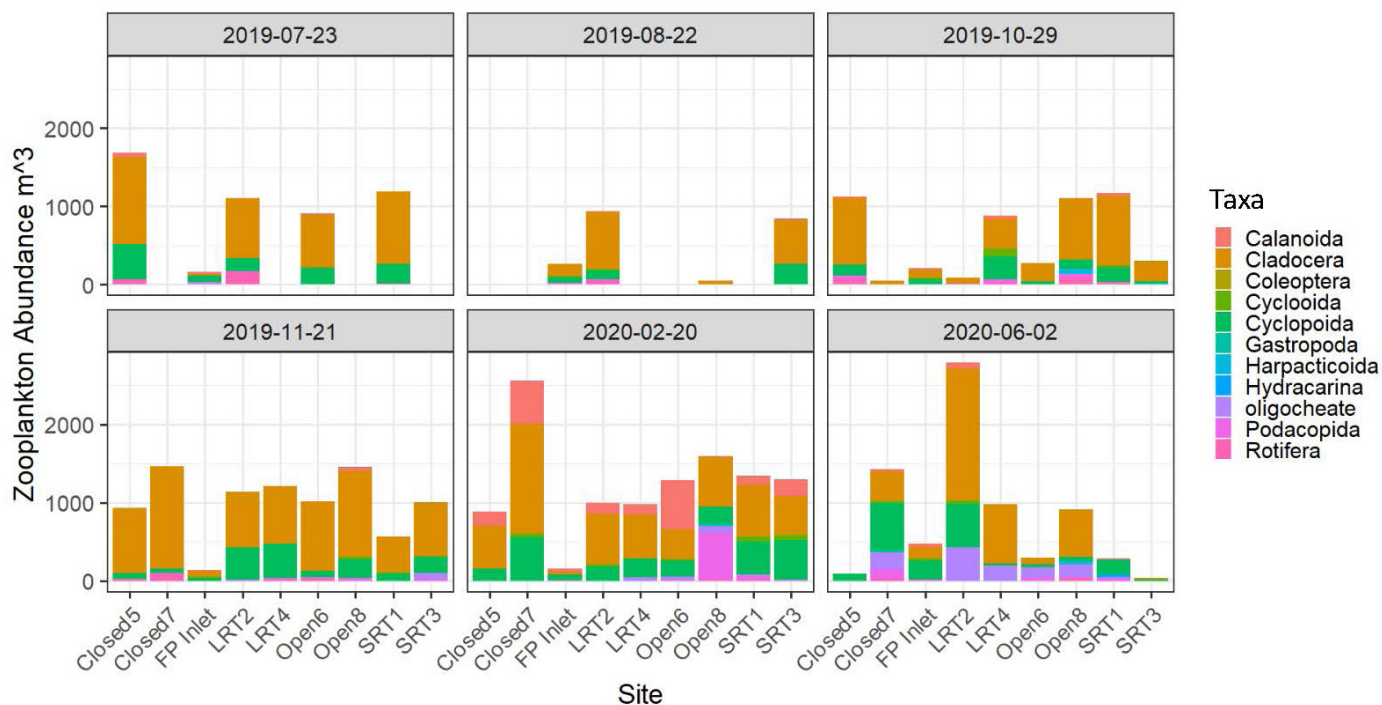
Figure 4 Stacked bar graphs of pelagic zooplankton abundance within the floating peat mesocosms for all quarterly sampling dates. SRT = short residence time, LRT = long residence time, Closed = full floating peat coverage, Open = half floating peat coverage, and FP Inlet = the adjacent South Fork Mokelumne River. Results for 2019-07-23 include only the pools that had peat blocks and received water. Closed7, LRT4, Open8, and SRT3 had yet to receive peat and be filled with water.

Temperature

For 77 days during June, July and August 2021, hourly temperatures were significantly lower at 110 cm and 15 cm in the mesocosms relative to the Mokelumne River at 110 cm (Figure 7). The mean Mokelumne River temperature at 110 cm was 24.2 °C and ranged from 21.2 to 26.7 °C. The mean mesocosm temperatures at 110 and 15 cm were 22.1 °C and 23.5 °C, and ranged from 18.8 to 24.6 °C, and 19.1 to 27.1 °C, respectively (Figure 7). Through shading, floating peat wetlands can potentially provide a lower-temperature refugia for fish.

Root Complexity

An extensive root complex grew below the peat blocks (Figure 8), which may have increased the area for biofilm for food for zooplankton. De Moraes et al. (2023) reported that extensive roots of floating wetlands increased the area for biofilm, which provided substrate for zooplankton and created structured habitats for fish at depths

of 0.5 to 0.8 m. De Moraes et al. (2023) also reported significantly higher numbers of captured fish associated with floating wetlands compared to a control, and that fish were attracted to floating wetlands root complexes for cover, shielding from aerial predators, and reduced light levels that inhibited predator vision—factors which are most important to juveniles. De Moraes et al. (2023) labeled the floating islands as a first step for helping juvenile fish growth within the protection of root complexity.

Biomass and Accretion

During 2020 and 2021, we measured an annual average increase of 1,560 g C m^{-2} in peat-block biomass (Table 2). Most of this carbon increase was belowground. The aboveground carbon productivity measured during this study was slightly greater than the range reported for the Twitchell West Pond wetland in Miller and Fujii (2010): 924 to 2,353 g dry weight m^{-2} or about 415 to 941 g C m^{-2}. The average dry bulk densities for
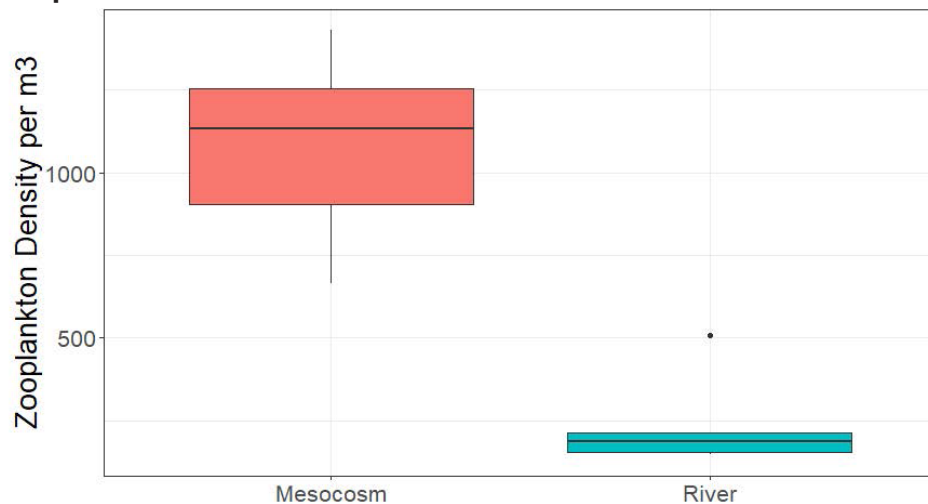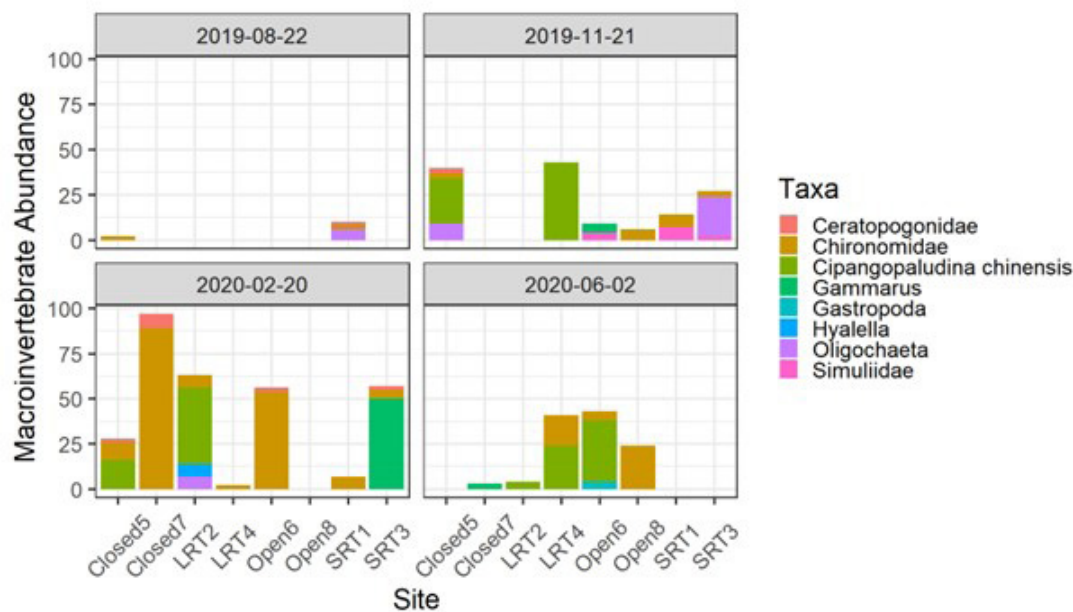
Zooplankton

Figure 6 Stacked bar graphs of macroinvertebrate abundance within the floating peat mesocosms for all quarterly sampling dates. SRT = short residence time, LRT = long residence time, Closed = full floating peat coverage, Open = half floating peat coverage.

the floating peat blocks were 0.068 g cm^{-3} in 2019 and 0.062 g cm^{-3} in 2021.

We compared our data with data reported for floating peats in the southeastern US. Sasser and Gosselink (1984) reported 1,960 g m^{-2} y^{-1} dry weight or about 980 g C m^{-2}y^{-1} (assuming a carbon content of 50%) net aboveground primary production in Louisiana floating peats. For comparison, the difference in aboveground

biomass between 2020 and 2021 for our floating peats was 471 g C m^{-2}y^{-1}, which represents net primary production (Table 3). Considering the standard deviation, data are consistent with Sasser and Gosselink (1984). For floating marshes in the lower Mississippi Delta, Izdepski et al. (2009) reported belowground biomass values that ranged from 472.7 to 4079.0 g m^{-2} or 236.4 to 2,039 g C m^{-2}, respectively. The belowground biomass estimate for this study was 1,089 g C m^{-2}.
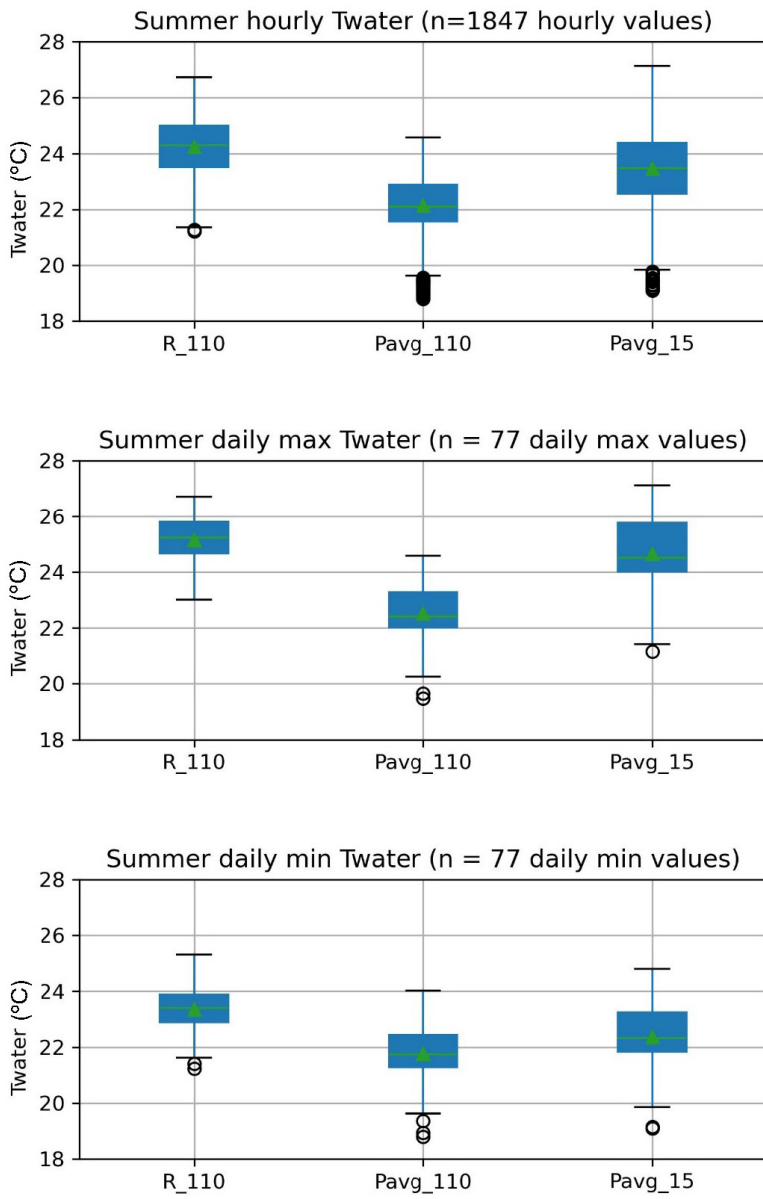
Figure 7 Boxplots of summer water temperature. R_110 denotes the Mokelumne River water temperature at 110 cm; Pavg_110 and Pavg_15 are the eight-pool average water temperatures at 110 cm depth and 15 cm depth, respectively. The *green triangles* represent mean temperatures. The *horizontal lines* within the *blue boxes* represent the median temperatures.

Figure 8 Photograph of underwater roots, January 2021

Table 2 Mean annual aboveground and belowground biomass for the eight mesocosms (n = 8) from years 2020 and 2021. We estimated the total biomass production from the difference. Data are available at *https://figshare.com/articles/dataset/Floating_Peat_Supplementary_Data/24775476.*

	Biomass (g C m^{-2} y^{-1})						
	2020 Harvest (n=8)			2021 Harvest (n=8)			Total biomass difference
	Above	**Below**	**Total**	**Above**	**Below**	**Total**	
Mean	1013.9	3448.8	4462.8	1485.3	4537.8	6023.1	1560.3
STDV	728	1893.7	—	829.3	1056	—	—

The higher value reported by Izdepski et al. (2009) was within the range measured during this study. Izdepski et al. (2009) aboveground biomass values ranged from 287.2 to 670 g C m^{-2} or 143.6 to 335 g C m^{-2} (Table 3). The higher value is within the range measured during this study. The robust root and rhizome systems of *Schoenoplectus* and *Typha* species (Drexler et al. 2018) likely contribute to the high productivity measured in the mesocosms.

Table 3 Comparison of aboveground floating wetland biomass estimates with those reported by Sasser and Gosselink (1984) and Ipenski et al. (2009)

This study estimated aboveground productivity (g C m^{-2} y^{-1}) (1485.3 minus 1013.9 from Table 2)	Sasser and Gosselink (1984) estimated aboveground productivity (g C m^{-2} y^{-1})	Izdepski et al. (2009) estimated aboveground productivity (g C m^{-2} y^{-1})
471	980	143.6–335

Using drone imagery from July 2019, we calculated an average of 45% initial areal peat-block coverage for the low-density, open-treatment mesocosms. Based on the drone imagery, floating peat coverage ranged from 67% to 79% in the open-treatment mesocosms during 2020–2022, and the average was 93% in closed treatment mesocosms. Using drone imagery from July 2019 to January 2022, we calculated a peat-block expansion rate of approximately 21% per year in the open-treatment mesocosms. In all mesocosms, peat blocks grew together to form large interwoven floating peat masses.

Biomass–NDVI–LAI relations were developed during 2020 and 2021 during biomass-sampling events (Figure 9A and 9B). Figure 9 indicates saturation of the LAI values above 4, which

is consistent with data presented in Asner et al. (2003) and Dronova and Taddeo (2016). The correlation between LAI and aboveground biomass supports the utility of LAI for estimating aboveground biomass accumulation for floating peats (Equation 9). Leaf area index values peaked in July 2020 and August 2021 (Figure 10). Vegetation senesced during the fall and winter, and LAI values were lowest in February 2021. The rapid increase in biomass production from late February to May 2021 corresponded to increasing air and water temperatures.

$$LAI = 0.5129 * - 17.446 * NDVI \ (R^2 = 0.71, \text{ p} < 0.001) \quad \textbf{Eq 8}$$

$$Aboveground\ Biomass = 473.99 * LAI - 636.31 \ (R^2 = 0.851, \text{ p} < .001) \quad \textbf{Eq 9}$$

Vertical accretion resulted primarily from organic matter accumulation. Accretion rates are meaningful for assessing the ability of the floating peats to remain stable over time and continue to float. The larger the volume of the submerged floating peat blocks, the greater the buoyant force and stability. With the average bulk density value of 0.062 g cm^{-3} from the eight mesocosms in 2021, and using the biomass accumulation between 2020 and 2021, we estimated an accretion rate of 5.5 cm yr^{-1} using Equation 10.

$$soil\ accretion_{field} = NCA * \frac{1}{BD} * \frac{2\ g\ Organic\ Matter}{1.1\ g\ Carbon} \quad \textbf{Eq 10}$$

where:

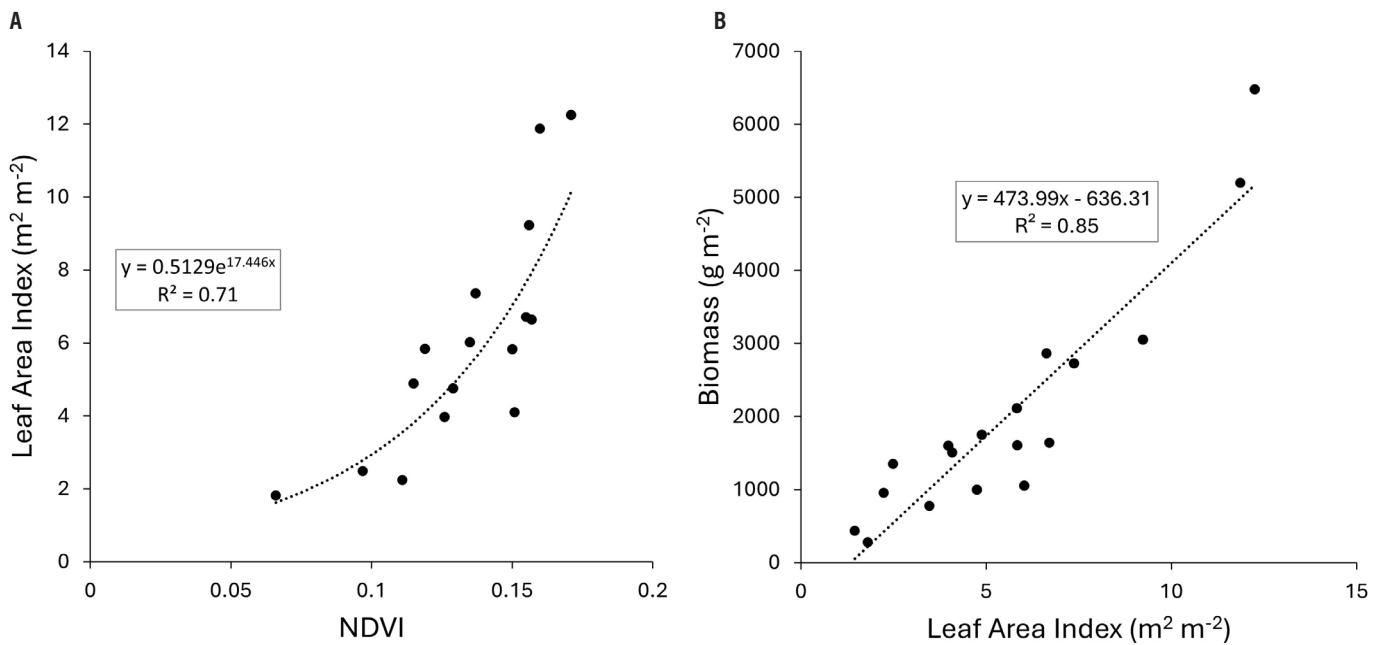*BD* is bulk density in g cm^{-3} and

A

B

Figure 9   Relationship of LAI to camera NDVI measured during Metropolitan Water District Program Manager Russell Ryan's drown flights (**A**) and of LAI to biomass (**B**). Data are available at *https://figshare.com/articles/dataset/Floating_Peat_Supplementary_Data/24775476*
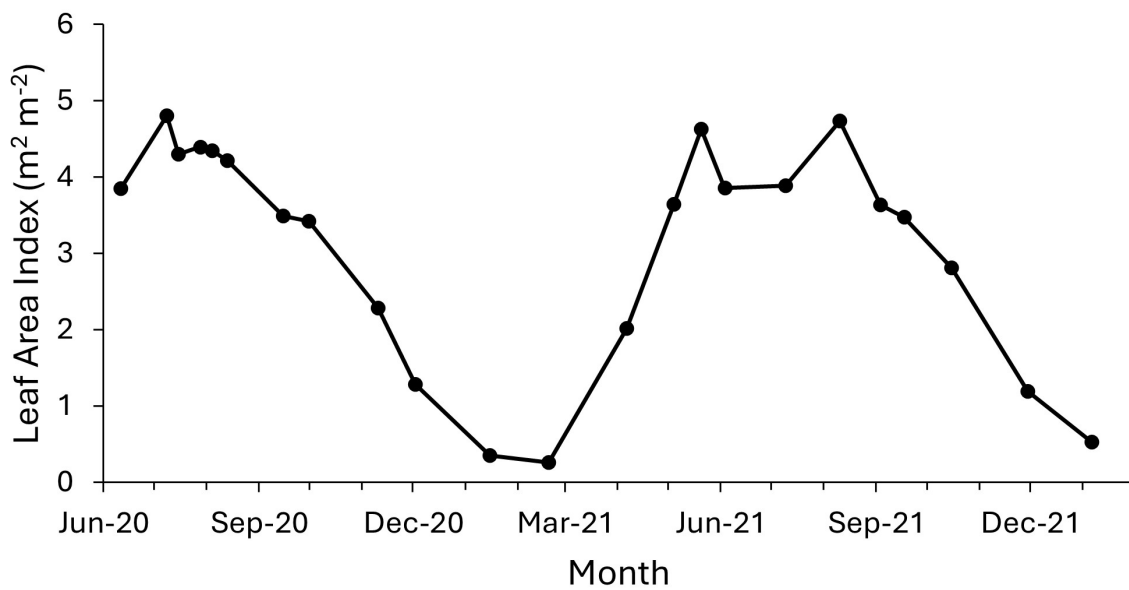

Figure 10   LAI calculated from the exponential relationship with camera NDVI (Equation 8 and Figure 9). Explanatory detail is provided in Appendix B, and data are available at *https://figshare.com/articles/dataset/Floating_Peat_Supplementary_Data/24775476*.

NCA is net carbon accumulation expressed in g C cm^{-2} yr^{-1}.

The relation of organic matter to organic carbon is based on data reported in Drexler et al. (2009).

This value is larger than the upper end of the range of 2.1 to 4.6 cm yr^{-1} reported by Miller et al. (2008) for the Twitchell West Pond wetland during 1997–2005. Deverel et al. (2020) reported 2.4 to 3 cm yr^{-1} of accretion during 1997 to 2017 for the Twitchell West Pond wetland. The 5.5 cm yr^{-1} is consistent with values for the Twitchell East End wetland, where Deverel et al. (2014) reported average rates of 7 cm yr^{-1} between 2003 and 2005, and 5.7 cm yr^{-1} between 2005 and 2008. Permanently flooded managed wetlands described in Miller et al. (2008) are accreting material under mostly permanently flooded and saturated conditions and are thus comparable with our measurements. The accreting material in the Twitchell West Pond and East End wetlands had a bulk density of generally less than 0.1 g cm^{-3}, and porosities ranged from 88% to 94% (Miller et al. 2008; Deverel et al. 2014).

In July 2019, the average peat-block thickness for all mesocosms was 44 cm, and ranged from 38 to 48 cm. The average of the September 2021 peat-block thicknesses for all mesocosms was 63 cm, and ranged from 53 to 72 cm. The average calculated difference for all mesocosms was 19 cm or 8.6 cm yr^{-1} and ranged from 3 to 12.5 cm yr^{-1}. This range is generally consistent with the range in the Twitchell West Pond and East Pond wetlands and the maximum annual accretion rate of 9.15 cm measured in the Twitchell East End wetland (Miller et al. 2008).

Our accretion rates and those reported by Miller et al. (2008) and Deverel et al. (2020) using sedimentation-erosion tables are higher than the rates Arias–Ortiz et al. (2021) reported for the Twitchell West Pond wetland (1.65 ± 0.54 cm yr^{-1}) based on Pb-210 dating of three 150-cm subsurface cores. The inconsistency may be due to uplifting of peat soil by emergent vegetation, which was observed in this wetland during the first decade after flooding. The Pb-210 dating method of age determination makes use of the ratio of the radioactive lead isotope Pb-210. Lead-210 results from the decay of radon-222 are useful for determining the ages of recent lacustrine and coastal marine sediments. The lead becomes attached to aerosols, which reach the Earth's surface either by dry fallout, or by being washed out of the atmosphere in precipitation. The upward scaffolding of underlying older organic deposits not affected by atmospheric lead-210 may have diluted the lead-210 signal.

Methane Fluxes

During flux measurements from July 2020 to January 2022 (Figure 11), we measured peat-block temperatures at 2 and 15 cm, and water temperatures at 15 cm below the surface (Figure 11). Methane flux variations varied concomitantly with temperature (Figures 11 and 12). Mesocosm and Mokelumne River temperatures varied from 8 °C to 27 °C. At 15 cm, mesocosm diurnal water temperatures varied as much as 2.5 °C. At 110 cm, diurnal temperatures varied by about +/– 0.5 °C.

We compared the relationships between peat-block fCH$_4$ and water and peat-block temperatures at 2 and 15 cm, by grouping the data in 3°C temperature classes (Figure 12). Using this grouping, peat-block temperature explained substantial temporal variation in fCH$_4$. The relationships between fCH$_4$ and soil and water temperatures at 2 and 15 cm were similar, as indicated in Equations 11, 12, and 13. Methane fluxes measured in short-residence-time treatment mesocosms were significantly lower than those measured in long-residence-time treatment mesocosms during April through October, when the medians were 70.2 nmol m^{-2} s^{-1} and 108.0 nmol m^{-2} s^{-1}, respectively (Figure 13).

The shorter residence time likely resulted in less reducing conditions (i.e., less capacity to generate methane) within the organic substrate, which is consistent with the aqueous CH$_4$ data described below. There was not a significant difference in fCH$_4$ between open and closed treatments.

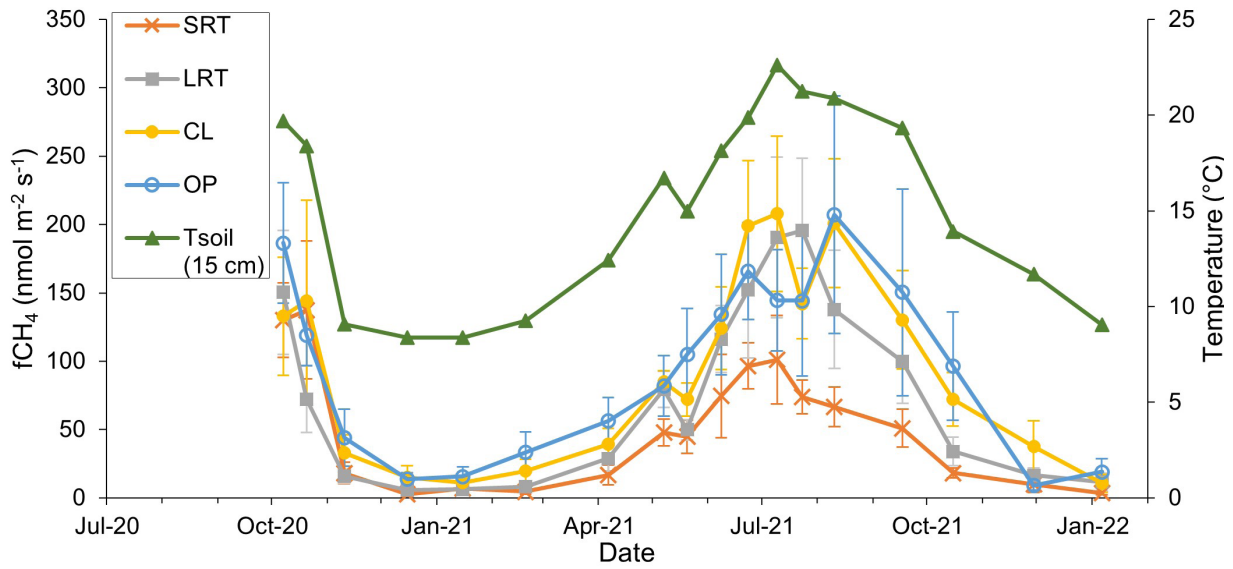**Figure 11** Temporal variability of CH_4 fluxes (fCH_4) for the four treatments and surface soil temperature, T_{soil} (15 cm). Treatments included SRT (short residence time), LRT (long residence time), CL (closed), and OP (open). Data are available at *https://figshare.com/articles/dataset/Floating_Peat_ Supplementary_Data/24775476*.
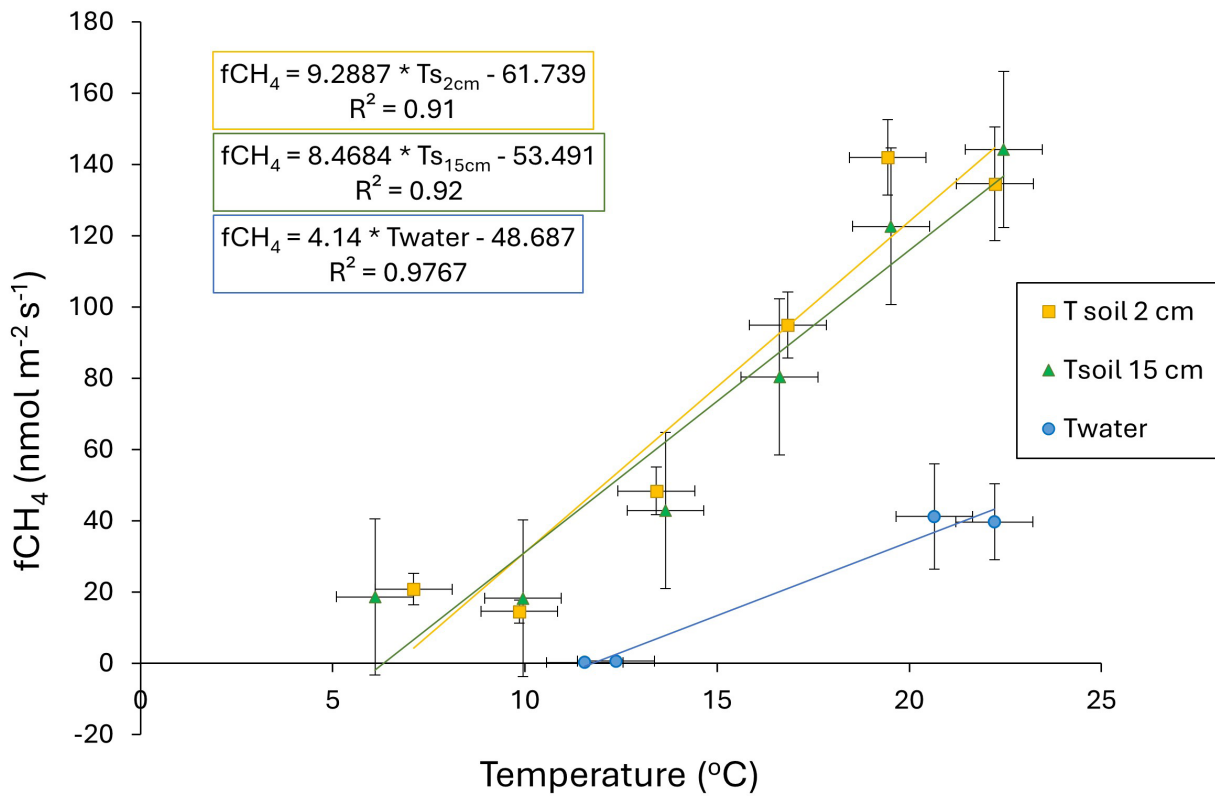

Figure 12 Relation of fCH_4 and pool surface-water temperature, and soil temperature at 2 and 15 cm between October 2020 and January 2022. We averaged flux measurements on the peat blocks using 3 °C temperature classes. The *error bars* represent the standard error. Data are available at *https://figshare.com/articles/dataset/Floating_Peat_Supplementary_Data/24775476*.

$$fCH_4 \ peat \ blocks = 9.29 * Tsoil_{2cm} - 61.739$$
$$(r^2 = 0.91, \ p = 0.0029) \qquad \textbf{Eq 11}$$

$$fCH_4 \ peat \ blocks = 8.47 * Tsoil_{15cm} - 53.491$$
$$(r^2 = 0.92, \ p = 0.0025) \qquad \textbf{Eq 12}$$

$$fCH_4 \ open \ water = 4.14 * Twater - 48.687$$
$$(r^2 = 0.98, \ p = 0.01) \qquad \textbf{Eq 13}$$

Using daily average temperature data grouped into 3-degree bins and Equation 11, we estimated the average daily and annual fCH_4 for peat blocks and open water (Table 4). We estimated the annual fCH_4 as the cumulative sum of estimated daily emissions using the temperature correlation. From September 2020 through August 2021, we estimated an annual fCH_4 for the open water of 7.3 t C m^{-2} (0.03 t C acre^{-1}), which is about 29% of the 25 g C m^{-2} (0.10 ton C acre^{-1}) estimated annual fCH_4 from the floating peats; which is equal to 3.84 metric ton CO$_2$eq acre^{-1} yr^{-1} using a Global Warming Potential (GWP) of 28 for 100 years (US EPA 2023). The annual fCH_4 value for the floating peats is lower than the other restored Delta impounded marshes (Hemes et al. 2019), and the value for the Dutch Slough Restoration Project's Gilbert Tidal Marsh (Table 5). For comparison, Arias–Ortiz et al. (2024) reported an average of 19.5 ± 40 g C m^{-2}year^{-1} for annual tidal wetland methane fluxes within the conterminous US.

Model Simulation Results

The PEPRMT-DAMM model (Oikawa et al. 2017) effectively simulated measured fCH_4 and fCO_2 (Figure 14 and Figures C1 and C2 in Appendix C, see "Data Accessibility Statement"). The root mean square error (RMSE) for fCH_4 was 0.0196 g C m^{-2}day^{-1}, thus indicating that the modeled values were within +/- 0.0196 g C m^{-2}day^{-1} or about +/-12% of measured values. The RMSE for fCO_2 was 1.108 g C m^{-2}day^{-1}, indicating that the modeled values estimated the measured values within +/- 1.108 g C m^{-2}day^{-1} or about +/- 16%.

Using a GWP of 28, the model-estimated average annual fCH_4 for the mesocosm peat blocks was 29 g C-CH$_4$ m^{-2}yr^{-1} or 4.38 metric

Table 4 Estimated average annual fCH_4 from peat blocks, open water, and mesocosms with partial or full cover of peat blocks

Unit	fCH_4 blocks	fCH_4 water	fCH_4 full-cover mesocosms	fCH_4 partial-cover mesocosms
g C m^{-2}	25	7.29	24	12
t C ha^{-1}	0.25	0.07	0.24	0.12

Table 5 Comparison of peat block fCH_4 values with fCH_4 values for restored wetlands in the Delta

Restored wetland	Annual CH$_4$ emissions g C m^{-2}	Reference
Sherman wetland	45.9 +/- 0.6	Hemes et al. (2019)
Twitchell East End wetland	31.8 +/- 13.7	Hemes et al. (2019)
Mayberry wetland	50.2 +/- 12.3	Hemes et al. (2019)
Twitchell West Pond wetland	45.4 +/- 9.0	Hemes et al. (2019)
Dutch Slough	31 +/- 5.0	LBNL https://ameriflux.lbl.gov/sites/siteinfo/US-Dmg
Floating peat	25.4 +/- 6.4	this study

ton CO$_2$-eq acre^{-1}yr^{-1}, consistent with the value of 25 g C-CH$_4$ m^{-2}yr^{-1} estimated using the temperature data described above and the value for the Gilbert Marsh, and lower than the average of vegetated Delta wetlands of 47 g C-CH$_4$ m^{-2}yr^{-1} (Hemes et al. 2019) (Table 5). Appendix C shows model inputs and sensitivity analysis results. Using the LAI estimated from NDVI as input to the model, we estimated that the floating peats were a net ecosystem carbon sink of – 820 +/– 137 g C m^{-2}yr^{-1}. This is a larger sink than the average of – 339 g C m^{-2}yr^{-1} for vegetated years for Sherman and Twitchell wetlands (Hemes et al. 2019) but consistent with the – 794 g C m^{-2}yr^{-1} +/– 30g C m^{-2}yr^{-1} for the UC Berkeley eddy covariance results for the Dutch Slough Restoration Project Gilbert Tidal Marsh (https://ameriflux.lbl.gov/sites/siteinfo/US-Dmg).

An analysis of the model's sensitivity demonstrated that the parameters governing fractional-absorbed photosynthetically active radiation and activation energy for the labile carbon pool were the primary model inputs, which—when varied—affected net ecosystem carbon exchange the most. Variations in
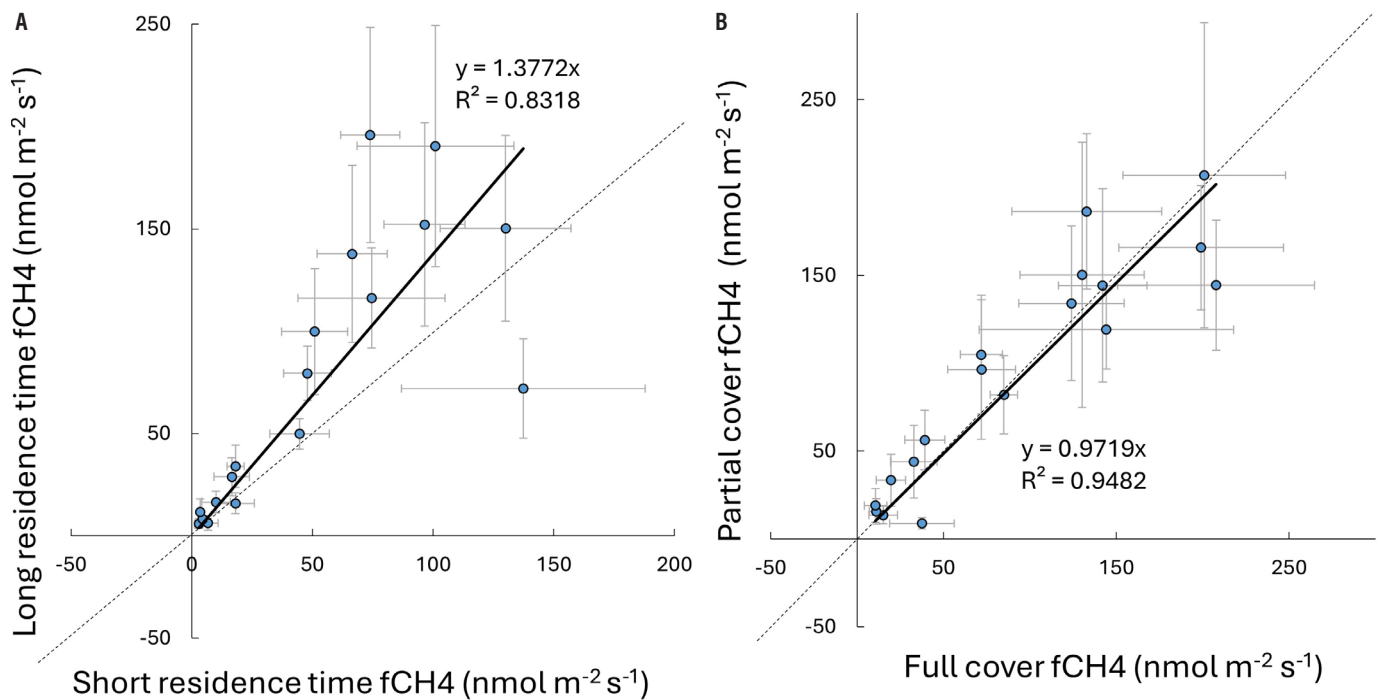
Figure 13   Comparison of fCH$_4$ for (**A**) short and long residence times (**A**) and of fCH$_4$ for (**B**) full (closed) and partial (open) peat-block cover (**B**). P-values for the residence time and pool coverage regression were <0.001. Data are available at *https://figshare.com/articles/dataset/Floating_Peat_Supplementary_Data/24775476*.
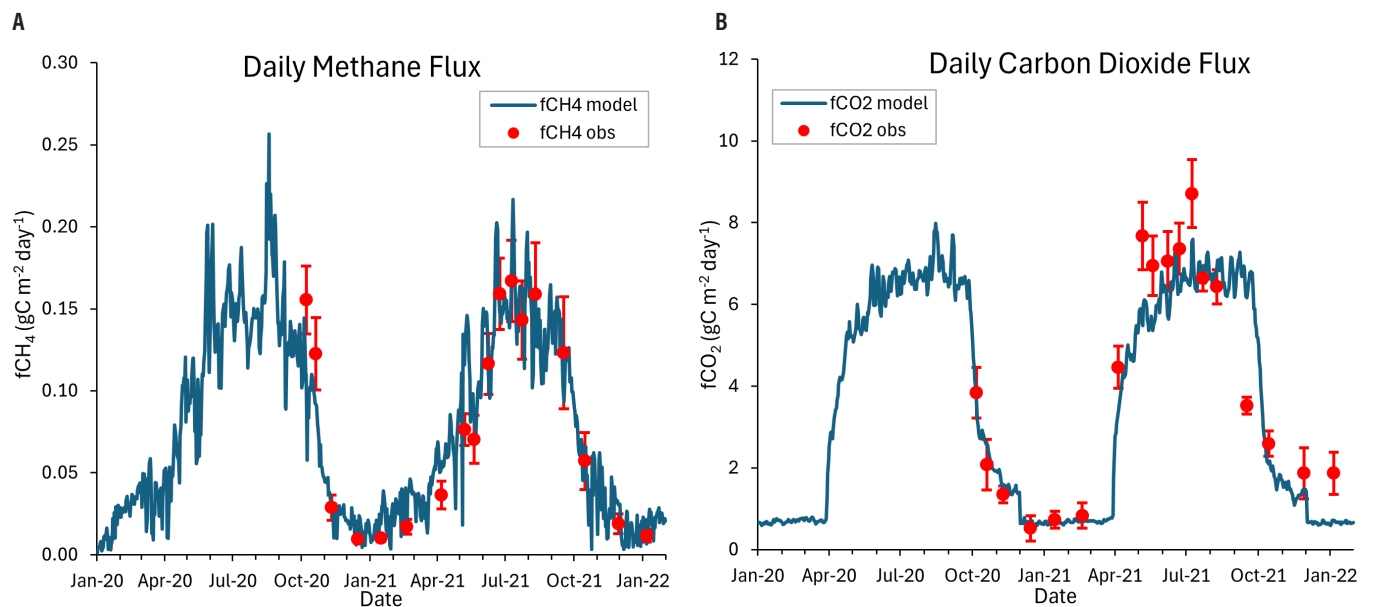

Figure 14   Time-series of (**A**) methane and (**B**) carbon dioxide fluxes. The *blue line* represents PEPRMT-model simulated daily fCH$_4$ or fCO$_2$. The *red dots* with *error bars* represent the average and standard error of fCH$_4$ and fCO$_2$ measurements from floating peat wetlands in all the mesocosms.

activation energies for CH_4 production and for CH_4 oxidation resulted in the largest changes in simulated CH_4 emissions.

Floating peats placed on oxidizing organic soils will likely be a net GHG sink over the long term. Two factors contribute: radiative forcing of CH_4 and long-term floatation. Hemes et al. (2019) and Arias–Ortiz et al. (2021) examined the cumulative radiative forcing of CH_4 and, using flux data for Delta wetlands, they calculated the crossover point: the time at which CO_2 sequestration completely offsets the cumulative atmospheric warming effects of emitted CH_4 and would manifest a net cooling relative to the baseline land use. The crossover point depended on baseline emissions and ranged from 30 to 89 years (Hemes et al. 2019; Arias–Ortiz et al. 2021). Long-term flotation is common for floating peats. For example, Hatton et al. (1983) summarized characteristics of floating marshes that included 30 years of growth and studied floating marshes that were over 100 years old. Accretion and expansion of the mesocosm peat blocks indicate future floatation stability. Moreover, Whipple et al. (2012) documented the robustness of Delta floating peat wetlands in their support of a herd of animals during flooding during the 19th century.

Water Quality
Elevated DO concentrations corresponded with low CH_4 concentrations. Before placement of peat blocks in the mesocosms in July 2019, CH_4 concentrations in mesocosm water samples averaged 0.3 ng L^{-1} (Figure 15). Results of the Mann–Whitney test indicated that CH_4 concentrations in the SRT mesocosms were significantly lower than those in the LRT mesocosms (p = 0.02). The median dissolved CH_4 concentrations for SRT and LRT mesocosms were 1.9 ug L^{-1} and 28.5 ug L^{-1}, respectively, over the full time-series from June 2020 through January 2022. Shorter residence times likely resulted in less reducing conditions in the floating-peat soil matrix, which, in turn, reduced methanogenesis relative to the LRT, and resulted in significantly lower fCH_4 values for the SRT mesocosms reported previously. Dissolved oxygen (DO) levels

followed a similar pattern, and levels in the mesocosms were consistently lower than those in the Mokelumne River. Mesocosm DO levels were lowest, generally less than 2 mg L^{-1}, during the summer and elevated during the winter (Figure D1 in Appendix D, see "Data Accessibility Statement").

Concentrations of major ions (calcium, magnesium, sodium, potassium, chloride, sulfate, and bicarbonate) for the mesocosms and the Mokelumne River remained similar throughout the course of the study. Mesocosm sulfate concentrations followed a trend nearly identical to the Mokelumne River, and values were similar. The presence of sulfate in the mesocosms may help explain the generally lower CH_4 emissions relative to other Delta wetlands (Table 5) and lower aqueous CH_4 concentrations in the short residence-time SRT mesocosms (Bartlett et al. 1987; Poffenbarger et al. 2011). Respiration via sulfate reduction is more thermodynamically favorable than respiration via methanogenesis, allowing sulfate-reducing bacteria to out-compete methanogenic archaea for resources when sulfate is available (He et al. 2015). Sulfate is reduced in Delta anoxic organic soils (Deverel et al. 1986). Arias–Ortiz (2024) reported an inverse relation between CH_4 fluxes and sulfate concentrations in tidal wetlands across the US.

Dissolved organic carbon (DOC) concentrations reflected a balance of wetland primary production and consumption by the microbial and invertebrate communities. Values for all treatments ranged from 1.3 to 4.9 mg L^{-1} during November 2019 to January 2022 (see Figure D2 in Appendix D), consistent with the Twitchell West Pond and East End wetlands where DOC concentrations ranged from 3 to 6 mg L^{-1} (Fleck et al. 2007). There was minimal POC in the mesocosm water.

Plant nitrogen uptake and denitrification (Richardson and Vepraskas 2001) probably resulted in lower nitrate concentrations in mesocosm samples compared with Mokelumne River samples (Figure D3 in Appendix D). Elevated mesocosm ammonia concentrations relative
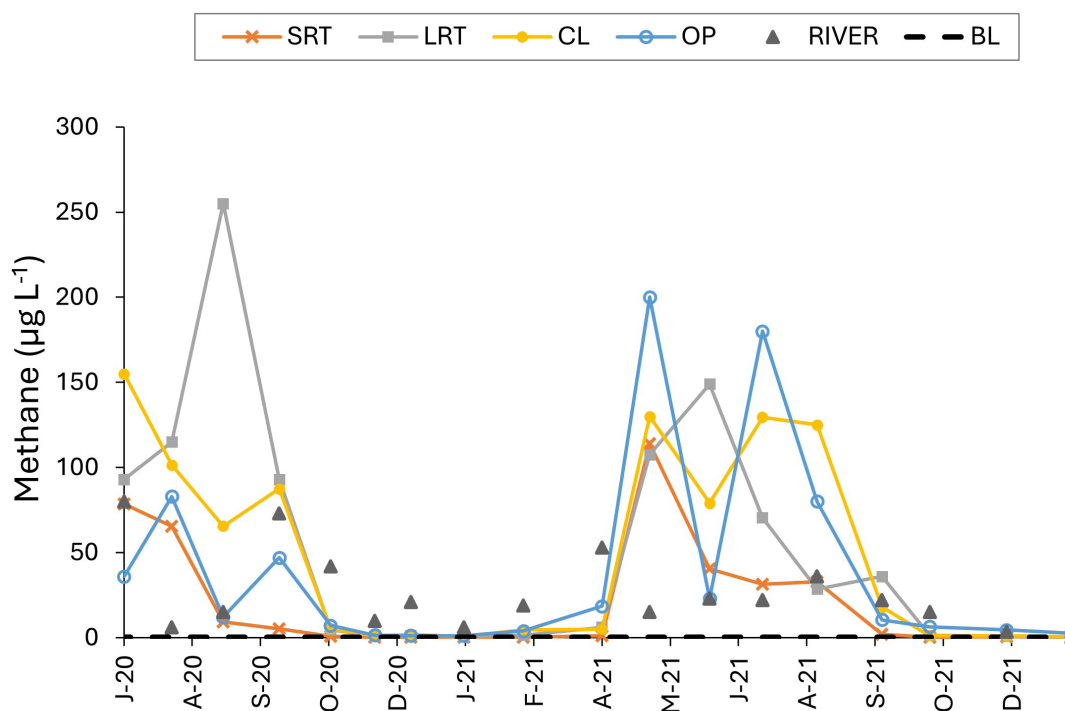
Figure 15 Average dissolved CH$_4$ concentrations for each treatment and the Mokelumne River vs. time from January 2020 through January 2022. The average baseline (BL) methane concentration was 0.3 ng L^{-1} measured in samples collected before peat-block placement and is represented by the *dashed black line*. Data are available at *https://figshare.com/articles/dataset/Floating_Peat_Supplementary_Data/24775476*.

to the Mokelumne River were likely the result of microbial conversion of organic nitrogen to ammonia (Richardson and Vepraskas 2001) or dissimilatory nitrate reduction (Scott et al. 2008).

Overall, Mokelumne River pH measurements were consistently higher than pH measured in the mesocosms. During March 2020 and January 2022, pH ranged between 6 and 7.5 pH for each treatment and ranged from 7 to 9 for the Mokelumne River. Lower pH values in the mesocosms compared with Mokelumne River are from biogeochemical processes that generate DOC and CO$_2$ and release organic acids from peat blocks. Deverel et al. (2007) reported median pH values that ranged from 5.5 to 6.58 in groundwater and drain water samples associated with organic soils on Twitchell Island.

All water quality data are available at *https://figshare.com/articles/dataset/Floating_Peat_Supplementary_Data/24775476.*

DISCUSSION

The primary potential ecosystem benefits of floating peat wetlands include increased food web, fish habitat, GHG emissions reductions, and subsidence reversal. Discussion is provided under the questions posed earlier.

What are the potential food-web and fish-habitat benefits?

Our results provide evidence that floating peat wetlands can provide biologically active organic matter that support zooplankton and macroinvertebrate populations at higher rates than the Mokelumne River. A combination of biologically available organic matter produced

Table 6   Summary of salient results

Topic	Salient results
Potential for food web and fish habitation	Zooplankton and macroinvertebrate data demonstrated the ability of the floating peats to support these populations, in the pelagic space between the benthos and the peat blocks, at levels greater than the Mokelumne River.
	Temperature data indicated that floating peat wetlands can potentially provide a lower-temperature refugia for fish.
	An extensive root complex, which could provide protective fish habitat, grew below the peat blocks in the mesocosms.
Biomass, accretion, and floatation	We measured net accumulation of 1.56 kg C m^{-2} from vegetation growth from 2020 to 2021.
	Horizonal expansion was 21% per year in the open mesocosms.
	Estimated average vertical accretion ranged from 5.5 to 8.6 cm yr^{-1}.
	Vertical accretion, horizontal expansion, and merging of wetland peat blocks result in increased buoyant force and indicate the potential for floatation in open waters.
Greenhouse gas emissions and removals and associated processes	The floating peats were a larger estimated net ecosystem carbon sink than the Sherman and Twitchell wetlands, but similar to the Dutch Slough Restoration Project's Gilbert Tidal Marsh.
	Shorter residence times resulted in lower methane emissions and aqueous methane concentrations during April through October.
Processes affecting water quality	Sulfate in the mesocosms likely contributed to lower methanogenesis relative to Delta terrestrial wetlands.
	Low nitrate and elevated ammonia concentrations in mesocosm samples relative to the Mokelumne River were likely the result of plant consumption, denitrification, dissimilatory nitrate reduction, and conversion of organic nitrogen to ammonia.

by native marsh as well as floodplain vegetation fueled the food webs in pre-development landscapes (Brown et al. 2016). Similar to our floating peats, these tidal wetlands were sufficiently anaerobic such that the build-up of organic material kept pace with sea level rise during the 6,000 years before the mid-19th century (Whipple et al. 2012). Food-web benefits were exported to adjacent surface waters.

Floating peat wetlands can provide a water-cooling effect. Davis et al. (2019) reported physiological stresses in Delta Smelt with elevated water temperatures, which can be exacerbated when food is limited. The combination of the increased zooplankton and macroinvertebrate production, and lower temperatures in the mesocosms relative to the Mokelumne River, thus indicate potential benefits for Delta Smelt and other species. Root complexity underlying floating peat wetlands can potentially provide habitation and protective benefits for juvenile fish (de Moraes et al. 2023).

What are the nature and effects of biomass accumulation and accretion?

Vertical accretion, horizontal expansion and growing together of the floating peat blocks increases stability, because the buoyant force on the peat blocks is proportional to the volume of water displaced. There is evidence in the scientific literature for long-term solidity and floatation of floating peats, including Delta floating peat islands. In the open-treatment mesocosms that were initially 45% open water, drone imagery demonstrated an expansion rate of 21% per year, thus indicating the potential for expansion of peat blocks placed in open-water areas. In March 2024, floating peat wetlands were placed without aboveground vegetation in the 10-hectare Bouldin Island West Pond. In September 2024, they continued to float in the face of windy conditions, and wetland vegetation had grown to about 2 m in height. Drone flights indicated horizontal expansion of about 9% from March to August 2024.

When placed on subsiding soils, the subsidence reversal benefit of floating peat wetlands will result from the inundation which stops the oxidation. This can also provide a levee-stability benefit. Decreasing peat thicknesses adjacent to levees increases seepage forces that can cause levee instability (Deverel et al. 2016). Creating a floating peat wetland adjacent to a levee reverses the effect of soil loss and reduces these seepage forces.

What are the GHG emissions and removals, and the processes and factors that affect these?

Our data indicate that the aqueous mesocosm environment resulted in substantial carbon sequestration and lower methane fluxes than in impounded marshes because of less reducing conditions, especially in the SRT treatment. Modeling served as a tool to integrate (1) estimation of the carbon balance and processes that affect GHG emissions and removals, and (2) calculation of a net ecosystem carbon balance. The floating peat block wetland is a larger carbon sink than the average for permanently-flooded, restored Delta wetlands on Twitchell and Sherman islands, but consistent with the value for the Dutch Slough Restoration Project's Gilbert Tidal Marsh. Water-quality data provided additional insight about methane fluxes.

What are the water-quality effects and processes?

The mesocosms altered aqueous methane, nitrogen, organic carbon, DO, and pH relative to the Mokelumne River. Within the mesocosms, significantly lower aqueous methane concentrations were associated with the SRTs. The SRT mesocosms also manifested slightly higher DO concentrations, which likely contributed to the statistically significantly lower aqueous methane concentrations and methane fluxes during April through October. Residence time likely influenced oxidation-reduction conditions in the peat blocks, and the presence of aqueous sulfate and DO likely contributed to lower methane emissions.

Dissolved oxygen concentrations measured in the mesocosms were not conducive to most Delta fish species. We posit that floating peats placed in a more hydrodynamically energetic environment will result in higher DO levels adjacent to the floating peats. Dissolved organic carbon concentrations in mesocosm samples were similar to concentrations measured in surface-water samples in the Twitchell West Pond and East End wetlands, indicating that organic carbon derived from aquatic vegetation released into surface water was consumed by mesocosm microflora and fauna. Future biogeochemical understanding will benefit from investigation of the carbon dynamics, especially as related to the aquatic food web, fish diets, and lateral carbon fluxes.

CONCLUSION

Our results point to potential additional experimentation directed toward answering questions about continued floatation, food web and fish benefits, and GHG emissions and removals in open-water environments. Floating peat wetlands in the Bouldin Island West Pond are being studied. Future implementation could include setback levee areas and parts of islands separated by cross levees such as a back channel between levees, similar to the Twitchell Island setback levee on the San Joaquin River (KSN Inc. 2016).

Additional questions and challenges include the following:

- How will floating peats behave in open water and tidally influenced areas? Similar field environmental data-collection methods to those used during this study, and additional data-collection efforts that include fish habitation, will be essential.

- What is the regional food-web and fish-habitat benefit? Additional data collection will help quantify the generation and export of fish food from floating peats in areas connected to Delta channels and quantify habitat benefits.

- Where will peat blocks for future experimentation and implementation come from? Removing large areas of peat blocks will present logistical and permitting challenges. Biologically supervised harvesting of peat blocks for this study demonstrated the feasibility of harvesting without detrimental effects in the wetland.

ACKNOWLEDGEMENTS

REFERENCES

Ahn C, Mitsch WJ. 2002. Scaling considerations of mesocosm wetlands in simulating large, created freshwater marshes. Ecol Eng. [accessed 2024 Sep 23];18(3):327–342.
https://doi.org/10.1016/S0925-8574(01)00092-1

Arias–Ortiz A, Wolfe J, Bridgham SD, Knox S, McNicol G, Needelman BA, Shahan J, Stuart–Haëntjens EJ, Windham–Myers L, Oikawa PY, et al. 2024. Methane fluxes in tidal marshes of the conterminous United States. Global Change Biology. [accessed 2024 Sep 26]:Sep;30(9):e17462.
https://doi.org/10.1111/gcb.17462

Arias–Ortiz A, Oikawa PY, Carlin J, Masqué P, Shahan J, Kanneg S, Paytan A, Baldocchi DD. 2021. Tidal and nontidal marsh restoration: a trade-off between carbon sequestration, methane emissions, and soil accretion. JGR Biogeosci. [accessed 2024 Sep 23];126(12):p.e2021JG006573.
https://doi.org/10.1029/2021JG006573

Asner GP, Scurlock JM, Hicke JA. 2003. Global synthesis of leaf area index observations: implications for ecological and remote sensing studies. Glob Ecol Biogeogr. [accessed 2024 Sep 23];12(3):191–205.
https://doi.org/10.1046/j.1466-822X.2003.00026.x

Atwater BF. 1980. Attempts to correlate late quaternary climatic records between San Francisco Bay, the Sacramento–San Joaquin Delta, and the Mokelumne River, California [dissertation]. [Newark (DE)]: University of Delaware. 214 p.

Bartlett KB, Bartlett DS, Harriss RC, Sebacher DI. 1987. Methane emissions along a salt marsh salinity gradient. Biogeochemistry. [accessed 2024 Sep 23];4:183–202.
https://doi.org/10.1007/BF02187365

Bianchette TA, Liu KB, Qiang Y, Lam, NSN. 2015. Wetland accretion rates along coastal Louisiana: spatial and temporal variability in light of Hurricane Isaac's impacts. Water. [accessed 2024 Sep 23];8(1):1.
https://doi.org/10.3390/w8010001

Blake GR, Hartge KH. 1986. Particle density. Methods of soil analysis: Part 1 physical and mineralogical methods. ASA-SSSA. 5:377–382.

Brown LR, Bennett WA, Wagner RW, Morgan–King T, Knowles N, Feyrer F, Schoellhamer DH, Stacey MT, Dettinger M. 2013. Implications for future survival of delta smelt from four climate change scenarios for the Sacramento–San Joaquin Delta, California. Estuaries Coasts 36:754–774.
http://doi.org/10.1007/s12237-013-9585-4

Brown LR, Kimmerer W, Conrad,JL, Lesmeister S, Mueller–Solger A. 2016. Food webs of the Delta, Suisun Bay, and Suisun Marsh: an update on current understanding and possibilities for management. San Franc Estuary Watershed Sci. [accessed 2024 Sep 23];14(3).
https://doi.org/10.15447/sfews.2016v14iss3art4

Byrd RH, Lu P, Nocedal, J, Zhu, C. 1995. A limited memory algorithm for bound constrained optimization. SIAM J Sci Comput. [accessed 2024 Sep 23];16(5):1190–1208.
https://doi.org/10.1137/0916069

[CDFW] California Department of Fish and Wildlife. 2020. Franks Tract Futures. [accessed 2024 Sep 23]. Available from:
https://franks-tract-futures-ucdavis.hub.arcgis.com/

Cloern JE, Safran SM, Vaughn LS, Robinson A, Whipple AA, Boyer KE, Drexler JZ, Naiman RJ, Pinckney JL, Howe ER, et al. 2021. On the human appropriation of wetland primary production. Sci. Total Environ. [accessed 2024 Sep 23];785:147097.
https://doi.org/10.1016/j.scitotenv.2021.147097

Corline NJ, Sommer T, Jeffres CA, Katz J. 2017. Zooplankton ecology and trophic resources for rearing native fish on an agricultural floodplain in the Yolo Bypass California, USA. Wetl Ecol Manag. [accessed 2024 Sep 23];25(5):533–545.
https://doi.org/10.1007/s11273-017-9534-2

Dachnowski–Stokes, AP. 1933. Grades of peat and muck for soil improvement (No. 290). Washington, DC: US Department of Agriculture. 31 p.

Davidson EA, Samanta S, Caramori SS, Savage K. 2012. The dual Arrhenius and Michaelis–Menten kinetics model for decomposition of soil organic matter at hourly to seasonal time scales. Glob Chang Biol. [accessed 2024 Sep 23];18(1):371–384.
https://doi.org/10.1111/j.1365-2486.2011.02546.x

Davidson EA, Savage KE, Finzi AC. 2014. A big-microsite framework for soil carbon modeling. Glob Chang Biol. [accessed 2024 Sep 23];20(12):3610–3620.
https://doi.org/10.1111/gcb.12718

Davis BE, Cocherell DE, Sommer T, Baxter RD, Hung, TC, Todgham AE, Fangue NA. 2019. Sensitivities of an endemic, endangered California smelt and two non-native fishes to serial increases in temperature and salinity: implications for shifting community structure with climate change. Conserv. Physiol. [accessed 2024 Sep 23];7(1):1–16.
https://doi.org/10.1093/conphys/coy076

de Moraes KR, Souza AT, Muška M, Hladík M, Čtvrtlíková M, Draštík V, Kolařík T, Kučerová A, Krolová M, Sajdlová Z, et al. 2023. Artificial floating islands: a promising tool to support juvenile fish in lacustrine systems. Hydrobiologia. [accessed 2024 Sep 23];850(9):1969–1984.
https://doi.org/10.1007/s10750-023-05204-8

Deverel SJ, Bachand S, Brandenberg SJ, Jones CE, Stewart JP, Zimmaro P. 2016. Factors and processes affecting delta levee system vulnerability. San Franc Estuary Watershed Sci. [accessed 2024 Sep 23];14(4).
https://doi.org/10.15447/sfews.2016v14iss4art3

Deverel SJ, Dore S, Schmutte C. 2020. Solutions for subsidence in the California Delta, USA, an extreme example of organic-soil drainage gone awry. Proc Int Assoc Hydrol Sci. [accessed 2024 Sep 23];382:837–842.
https://doi.org/10.5194/piahs-382-837-2020

Deverel SJ, Ingrum T, Leighton DA. 2016. Present-day oxidative subsidence of organic soils and mitigation in the Sacramento–San Joaquin Delta, California, USA. Hydrogeol J. [accessed 2024 Sep 23];24(3):569–586.
https://doi.org/10.1007/s10040-016-1391-1

Deverel SJ. Ingrum T, Lucero C, Drexler JZ. 2014. Impounded marshes on subsided islands: simulated vertical accretion, processes, and effects, Sacramento-San Joaquin Delta, CA USA. San Franc Estuary Watershed Sci. [accessed 2024 Sep 23];12(2).
https://doi.org/10.15447/sfews.2014v12iss2art5

Deverel SJ, Leighton, David A, Finlay, Mark R. 2007. Processes affecting agricultural drainwater quality and organic carbon loads in California's Sacramento–San Joaquin Delta. San Franc Estuary Watershed Sci. [accessed 2024 Sep 23];5(2).
https://doi.org/10.15447/sfews.2007v5iss2art2

Deverel SJ, Whittig LD, Tanji KK. 1986. Sulfate reduction and calcium carbonate equilibria in a Central California histosol. Soil Sci Soc Am J. [accessed 2024 Sep 23];50(5):1189–1193. *https://doi.org/10.2136/sssaj1986.03615995005000050019x*

Drexler JZ, de Fontaine CS, Brown TA. 2009. Peat accretion histories during the past 6,000 years in marshes of the Sacramento–San Joaquin Delta, CA, USA. Estuaries Coasts. [accessed 2024 Sep 23];32(5):871–892.
https://doi.org/10.1007/s12237-009-9202-8

Drexler JZ, Khanna S, Schoellhamer DH, Orlando J. 2018. The fate of blue carbon in the Sacramento–San Joaquin Delta of California, USA. In: Windham-Myers L, Crooks S, Troxler TG, editors. A Blue carbon primer. [unknown]: CRC Press. p. 307–325.

Dronova I, Taddeo S. 2016. Canopy leaf area index in non-forested marshes of the California Delta. Wetlands. [accessed 2024 Sep 23];36:705–716. https://doi.org/10.1007/s13157-016-0780-5

Durand JR. 2017. Evaluating the aquatic habitat potential of flooded polders in the Sacramento–San Joaquin Delta. San Franc Estuary Watershed Sci. [accessed 2024 Sep 23];15(4). https://doi.org/10.15447/sfews.2017v15iss4art4

Ederington MC, McManus GB, Harvey HR. 1995. Trophic transfer of fatty acids, sterols, and a triterpenoid alcohol between bacteria, a ciliate, and the copepod *Acartia tonsa*. Limnol Oceanogr. [accessed 2024 Sep 23];40(5):860–867. https://doi.org/10.4319/lo.1995.40.5.0860

Fleck JA, Fram MS, Fujii R. 2007. Organic carbon and disinfection byproduct precursor loads from a constructed, non-tidal wetland in California's Sacramento–San Joaquin Delta. San Franc Estuary Watershed Sci. [accessed 2024 Sep 23];5(2). https://doi.org/10.15447/sfews.2007v5iss2art1

Folse TM, McGinnis TE, Sharp LA, West JL, Hymel, MK, Troutman JP, Weifenbach D, Boshart WM, Rodrigue LB, Richardi DC, Wood WB, 2020. A standard operating procedures manual for the coastwide reference monitoring system-wetlands and the system-wide assessment and monitoring program: methods for site establishment, data collection, and quality assurance/quality control. Baton Rouge (LA): Louisiana Coastal Protection and Restoration Authority. 252 p.

Gamon JA. 2015. Reviews and syntheses: optical sampling of the flux tower footprint. Biogeosciences. [accessed 2024 Sep 23];12(14):4509–4523. https://doi.org/10.5194/bg-12-4509-2015

Hanley J. 2020. Ecology and classification of North American freshwater invertebrates. [accessed 2020 Apr 16]. Available from: http://cfb.unh.edu/cfbkey/html/

Hargis TG, Twilley RR. 1994. Improved coring device for measuring soil bulk density in a Louisiana deltaic marsh. J Sediment Res. [accessed 2024 Sep 23];64(3):681–683. https://doi.org/10.1306/D4267E60-2B26-11D7-8648000102C1865D

Hatton RS, DeLaune RD, Patrick Jr WH. 1983. Sedimentation, accretion, and subsidence in marshes of Barataria Basin, Louisiana. Limnol Oceanogr. [accessed 2024 Sep 23];28(3):494–502. https://doi.org/10.4319/lo.1983.28.3.0494

He Q, Yang H, Wu L, Hu, C. 2015. Effect of light intensity on physiological changes, carbon allocation and neutral lipid accumulation in oleaginous microalgae. Bioresour Technol. [accessed 2024 Sep 23];191:219–228. https://doi.org/10.1016/j.biortech.2015.05.021

Helsel DR, Hirsch RM. 2002. Chapter A3: Statistical methods in water resources, techniques of water-resources investigations of the United States Geological Survey. In: US Geological Survey. 2002. Book 4, Hydrologic Analysis and Interpretation. [accessed 2024 Sep 23]. Reston (VA): US Geological Survey. 522 p. Available from: http://water.usgs.gov/pubs/twri/twri4a3/

Hemes KS, Chamberlain SD, Eichelmann E, Anthony T, Valach A, Kasak K, Szutu D, Verfaillie J, Silver WL, Baldocchi DD. 2019. Assessing the carbon and climate benefit of restoring degraded agricultural peat soils to managed wetlands. Agr Forest Meteorol. [accessed 2024 Sep 23];268:202–214. https://doi.org/10.1016/j.agrformet.2019.01.017

Hobbs RJ, Arico S, Aronson J, Baron JS, Bridgewater P, Cramer VA, Epstein PR, Ewel JJ, Klink CA, Lugo AE, et al. 2006. Novel ecosystems: theoretical and management aspects of the new ecological world order. Glob Ecol Biogeogr. [accessed 2024 Sep 23];15(1):1–7. https://doi.org/10.1111/j.1466-822X.2006.00212.x

Holm Jr GO, Sasser CE, Peterson GW, Swenson EM. 2000. Vertical movement and substrate characteristics of oligohaline marshes near a high-sediment, riverine system. J Coast Res. [accessed 2024 Sep 23];16(4):164–171. Available from: https://journals.flvc.org/jcr/article/view/80785/77943

Howe ER, Simenstad CA, Toft JD, Cordell JR, Bollens SM. 2014. Macroinvertebrate prey availability and fish diet selectivity in relation to environmental variables in natural and restoring north San Francisco bay tidal marsh channels. San Franc Estuary Watershed Sci. [accessed 2024 Sep 23];12(1). *https://doi.org/10.15447/sfews.2014v12iss1art5*

Hutchinson GL, Livingston GP. 2001. Vents and seals in non-steady-state chambers used for measuring gas exchange between soil and the atmosphere. Eur J Soil Sci. [accessed 2024 Sep 23];52(4):675–682. *https://doi.org/10.1046/j.1365-2389.2001.00415.x*

Izdepski CW, Day JW, Sasser CE, Fry B. 2009. Early floating marsh establishment and growth dynamics in a nutrient amended wetland in the lower Mississippi Delta. Wetlands. [accessed 2024 Sep 23];29(3):1004–1013. *https://doi.org/10.1672/08-218.1*

Jassby AD, Cloern JE. 2000. Organic matter sources and rehabilitation of the Sacramento–San Joaquin Delta (California, USA). Aquatic Conserv: Mar Freshw Ecosyst. [accessed 2024 Sep 23];10(5):323–352. *https://doi.org/10.1002/1099-0755(200009/10)10:5<323::AID-AQC417>3.0.CO;2-J*

Jassby AD, Cloern JE, Mueller–Solger AB. 2003. Phytoplankton fuels Delta food web. Calif Agric. [accessed 2024 Sep 23];57(4):104–109. *https://doi.org/10.3733/ca.v057n04p104*

Kimmerer WJ, Orsi J. 1996. Changes in the zooplankton of the San Francisco Bay Estuary since the introduction of the clam *Potamocorbula amurensis*. In: Hollibaugh J, editor. 1996. San Francisco Bay: the ecosystem. San Francisco (CA): AAAS, Pacific Division. p. 403–424. Available from: *https://www.google.com/url?sa=t&rct=j&q=&esrc=s&source=web&cd=&ved=2ahUKEwjn__H7u4yKAxW9DjQIHUpWJXYQFnoECA8QAQ&url=https%3A%2F%2Fdownloads.regulations.gov%2FFWS-R8-ES-2022-0082-0003%2Fattachment_29.pdf&usg=AOvVaw1QItOxFw1aI6M5nHznrtaa&opi=89978449*

KSN Inc. 2016. Resilience through restoration: Reclamation District No. 1601 Twitchell Island San Joaquin River setback levee project. [accessed 2024 Sep 23]. Available from: *https://cdn.ymaws.com/membersfloodplain.site-ym.com/resource/resmgr/2016Conference/Twitchell_Island.pdf*

Knox SH, Dronova I, Sturtevant C, Oikawa PY, Matthes JH, Verfaillie J, Baldocchi D. 2017. Using digital camera and Landsat imagery with eddy covariance data to model gross primary production in restored wetlands. Agric For Meteorol. [accessed 2024 Sep 23];237:233–245. *https://doi.org/10.1016/j.agrformet.2017.02.020*

Lamers LPM, Farhoush C, Van Groenendael JM, Roelofs JGM. 1999. Calcareous groundwater raises bogs; the concept of ombrotrophy revisited. J Ecol. [accessed 2024 Sep 23];87(4):639–648. *https://doi.org/10.1046/j.1365-2745.1999.00380.x*

[LBNL] Lawrence Berkeley National Laboratory. Ameriflux Management Project. [accessed 2024 Sep 23]. Available from: *https://ameriflux.lbl.gov/login/?redirect_to=/data/download-data/*

Livingston GP, Hutchinson GL. 1995. Enclosure-based measurement of trace gas exchange: applications and sources of error. In: Matson PA, Harriss RC, editors. Biogenic trace gases: measuring emissions from soil and water. Oxford (UK): Blackwell Science Ltd. p 14–51. Available from: *https://books.google.com/books?id=WDjpgK7IQAgC&pg=PA14&source=gbs_toc_r&cad=2#v=onepage&q&f=false*

Lott J. 1998. Feeding habits of juvenile and adult delta smelt from the Sacramento–San Joaquin River Estuary. Interagency Ecological Program Newsletter. [accessed 2024 Sep 23];11(1):14–19. Available from: *https://www.waterboards.ca.gov/waterrights/water_issues/programs/bay_delta/california_waterfix/exhibits/docs/COSJ%20et%20al/part2sur_rebuttal/SJC_461.pdf*

Mallison CT, Stocker RK, Cichra CE. 2001. Physical and vegetative characteristics of floating islands. J Aquat Plant Manage. [accessed 2024 Sep 23];39:107–111. Available from: *https://apms.org/wp-content/uploads/japm-39-02-107.pdf*

Matson PA, Harriss RC, editors. 2009. Biogenic trace gases: measuring emissions from soil and water. Cambridge (MA): Blackwell Science. 408 p.

Merritt RW, Cummins KW, Berg MB, editors. 2008. An introduction to the aquatic insects of North America. 4th ed. Dubuque (IA): Kendall/Hunt Publishing Company. 1158 p.

Miller R, Fujii, R. 2010. Plant community, primary productivity, and environmental conditions following wetland re-establishment in the Sacramento–San Joaquin Delta, California. Wetlands Ecol Manage. [accessed 2024 Sep 23];18:1–16. *https://doi.org/10.1007/s11273-009-9143-9*

Miller RL, Fram MS, Fujii R, Wheeler G. 2008. Subsidence reversal in a re-established wetland in the Sacramento–San Joaquin Delta, California, USA. San Franc Estuary Watershed Sci. [accessed 2024 Sep 23];6(3). *https://doi.org/10.15447/sfews.2008v6iss3art1*

Mosier AC, Francis CA. 2008. Relative abundance and diversity of ammonia-oxidizing archaea and bacteria in the San Francisco Bay estuary. Environ Microbiol. [accessed 2024 Sep 23];10(11):3002–3016. *https://doi.org/10.1111/j.1462-2920.2008.01764.x*

Mount J, Twiss R. 2005. Subsidence, sea level rise, and seismicity in the Sacramento–San Joaquin Delta. San Franc Estuary Watershed Sci. [accessed 2024 Sep 23];3(1). *https://doi.org/10.15447/sfews.2005v3iss1art7*

Moyle PB, Herbold B, Stevens DE, Miller LW. 1992. Life history and status of delta smelt in the Sacramento-San Joaquin Estuary, California. Trans Am Fish Soc. [accessed 2024 Sep 23];121(1):67–77. *https://doi.org/10.1577/1548-8659(1992)121<0067:LHASOD>2.3.CO;2*

Moyle PB. 2002. Inland fishes of California: revised and expanded. Berkeley (CA): University of California Press. [accessed 2024 Sep 23]. 413 p. Available from: *https://www.waterboards.ca.gov/water_issues/programs/tmdl/records/state_board/1998/ref2608.pdf*

Moyle PB, Leidy RA. 1992. Loss of biodiversity in aquatic ecosystems: evidence from fish faunas. In: Fiedler PL, Jain SK, editors. Conservation biology: the theory and practice of nature conservation preservation and management. Boston (MA): Springer US. [accessed 2024 Sep 24]. p.127–169. Available from: *https://doi.org/10.1007/978-1-4684-6426-9_6*

Nelson DW, Sommers LE. 1996. Total carbon, organic carbon, and organic matter. In: Bartels JM, et al. editors. Methods of soil analysis: Part 3 Chemical methods. 3rd ed. Book series no. 5. p.961–1010. Madison (WI): ASA and SSSA.

Nobriga ML. 2002. Larval Delta smelt diet composition and feeding incidence: environmental and ontogenetic influences. Calif Fish Game. [accessed 2024 Sep 24];88(4):149–164. Available from: *https://www.researchgate.net/profile/Matthew-Nobriga/publication/279191627_Larval_Delta_Smelt_Diet_Composition_and_Feeding_Incidence_Environmental_and_Ontogenetic_Influences/links/558d717408ae47a3490bc5f2/Larval-Delta-Smelt-Diet-Composition-and-Feeding-Incidence-Environmental-and-Ontogenetic-Influences.pdf*

Northwest Hydraulic Consultants. 2006. Assessment of sediment budget of Sacramento-San Joaquin Delta. Report for the California Department of Water Resources. Sacramento (CA): California Department of Water Resources. 36 p.

Nyman JA, Walters RJ, Delaune RD, Patrick Jr WH. 2006. Marsh vertical accretion via vegetative growth. Estuarine Coast Shelf Sci. 69(3-4):370-380.

Oikawa PY, Jenerette GD, Knox SH, Sturtevant C, Verfaillie J, Dronova I, Poindexter CM, Eichelmann E, Baldocchi DD. 2017. Evaluation of a hierarchy of models reveals importance of substrate limitation for predicting carbon dioxide and methane exchange in restored wetlands. JGR Biogeosci. [accessed 2024 Sep 24];122(1):145–167. *https://doi.org/10.1002/2016JG003438*

Opperman JJ, Galloway GE, Fargione J, Mount JF, Richter BD, Secchi S. 2009. Sustainable floodplains through large-scale reconnection to rivers. Science. [accessed 2024 Sep 24];326(5959):1487–1488. *https://doi.org/10.1126/science.1178256*

Parkin TB, Venterea RT. 2010. Chapter 3. Chamber-based trace gas flux measurements. In: USDA-ARS GRACEnet project protocols. Sampling protocols. Beltsville (MD): RF Follett. [accessed 2024 Sep 24]. p. 1–39. Available from: *https://www.ars.usda.gov/ARSUserFiles/np212/chapter%203.%20gracenet%20Trace%20Gas%20Sampling%20protocols.pdf*

Pavelka M, Acosta M, Kiese R, Altimir N, Brümmer C, Crill P, Darenova E, Fuß R, Gielen B, Graf A, et al. 2018. Standardization of chamber technique for CO_2, N_2O and CH_4 flux measurements from terrestrial ecosystems. Int Agrophys. [accessed 2024 Sep 24];32(4):569–587. *https://doi.org/10.1515/intag-2017-0045*

Poffenbarger HJ, Needelman BA, Megonigal JP. 2011. Salinity influence on methane emissions from tidal marshes. Wetlands. [accessed 2024 Sep 24];31(5):831–842. *https://doi.org/10.1007/s13157-011-0197-0*

R Core Team. 2022. R: a language and environment for statistical computer (Version 4.1.3). Vienna (Austria): R Foundation for the Statistical Computing. [accessed 2024 Sep 24]. Available from: *https://www.R-project.org/*

Richardson JL, Vepraskas MJ. 2001. Wetland soils: genesis, hydrology, landscapes, and classification. Boca Raton (FL): Lewis Publishers. p.98-100.

Robinson A, Richey A, Cloern JE, Boyer KE, Burau J, Canuel EA, DeGeorge JF, Drexler JZ, Howe ER, Kneib R, et al. 2016. Primary production in the Sacramento–San Joaquin Delta: a science strategy to quantify change and identify future potential. Richmond (CA): San Francisco Estuary–Aquatic Science Center. [accessed 2024 Sep 24]. Available from: *https://www.sfei.org/sites/default/files/biblio_files/DPPW%20Combined%20Rev%202019_05_20.pdf*

Ruimy A, Kergoat L, Bondeau A, The Participants of the Potsdam NpP Model Intercomparison Intercomparison, T.P.O.T.P.N.M. 1999. Comparing global models of terrestrial net primary productivity (NPP): analysis of differences in light absorption and light-use efficiency. Glob Chang Biol. [accessed 2024 Sep 24];5(S1):56–64. *https://doi.org/10.1046/j.1365-2486.1999.00007.x*

Russell RJ. 1942. Flotant. Geogr Rev. [accessed 2024 Sep 24];32(1):74-98. *https://doi.org/10.2307/210360*

Sasser CE, Gosselink JG. 1984. Vegetation and primary production in a floating freshwater marsh in Louisiana. Aquat Bot. [accessed 2024 Sep 24];20(3–4):245–255. *https://doi.org/10.1016/0304-3770(84)90090-1*

Sasser CE, Gosselink JG, Swenson EM, Swarzenski CM, Leibowitz NC. 1996. Vegetation, substrate and hydrology in floating marshes in the Mississippi river delta plain wetlands, USA. Vegetatio. [accessed 2024 Sep 24];122(2)129–142. *https://doi.org/10.1007/BF00044695*

Salimi S, Almuktar SA, Scholz M. 2021. Impact of climate change on wetland ecosystems: a critical review of experimental wetlands. J Environ Manag. [accessed 2024 Sep 24];286:112160. *https://doi.org/10.1016/j.jenvman.2021.112160*

Scott JT, McCarthy MJ, Gardner WS, Doyle RD. 2008. Denitrification, dissimilatory nitrate reduction to ammonium, and nitrogen fixation along a nitrate concentration gradient in a created freshwater wetland. Biogeochemistry. [accessed 2024 Sep 24];87:99–111. *https://doi.org/10.1007/s10533-007-9171-6*

Sihi D, Davidson EA, Savage KE, Liang D. 2019. Simultaneous numerical representation of soil microsite production and consumption of carbon dioxide, methane, and nitrous oxide using probability distribution functions. Glob Chang Biol. [accessed 2024 Sep 24]26:200–218. *https://doi.org/10.1111/gcb.14855*

Smolders AJP, Tomassen HBM, Lamers LPM, Lomans BP, Roelofs JGM. 2002. Peat bog restoration by floating raft formation: the effects of groundwater and peat quality. J Appl Ecol. [accessed 2024 Sep 24];39(3):391–401. *https://doi.org/10.1046/j.1365-2664.2002.00724.x*

Swarzenski CM, Swenson EM, Sasser CE, Gosselink JG. 1991. Marsh mat flotation in the Louisiana delta plain. J Ecol. [accessed 2024 Sep 24];79(4)999–1011. *https://doi.org/10.2307/2261094*

Thorp JH, Covich AP, editors. 2009. Ecology and classification of North American freshwater invertebrates. 3rd Ed. Academic Press. [accessed 2024 Sep 24]. Available from: *https://www.sciencedirect.com/book/9780123748553/ecology-and-classification-of-north-american-freshwater-invertebrates*

Tomassen HBM, Smolders AJP, Lamers LPM, Roelofs JGM. 2004. Development of floating rafts after the rewetting of cut-over bogs: the importance of peat quality. Biogeochemistry. [accessed 2024 Sep 24];71(1):69–87. *https://doi.org/10.1007/s10533-004-3931-3*

van Donselaar-ten Bokkel Huinink WAE. 1961. An ecological study of the vegetation in three former riverbeds. Wentia. [accessed 2024 Sep 24];5(1):112–162. Available from: *https://repository.naturalis.nl/pub/535174/MBMHU1961174001001.pdf*

[USEPA] US Environmental Protection Agency. 2023. Understanding global warming potentials. [accessed 2024 Sep 24]. Available from: *https://www.epa.gov/ghgemissions/understanding-global-warming-potentials*

Vaughn LJ, Deverel SJ, Panlasigui S, Drexler JZ, Olds MA, Díaz JT, Harris KF, Morris J, Grenier JL, Robinson AH, et al. 2024. Managed wetlands for climate action: potential greenhouse gas and subsidence mitigation in the Sacramento–San Joaquin Delta. San Franc Estuary Watershed Sci. [accessed 2024 Sep 24];22(2). *https://doi.org/10.15447/sfews.2024v22iss2art3*

Volkova EM. 2010. The way of floating peat formation in karst depressions of European Russia. Open Geogr J. [accessed 2024 Sep 24];3(1):67–72. *https://doi.org/10.2174/1874923201003010067*

Wagner RW, Stacey M, Brown LR, Dettinger M. 2011. Statistical models of temperature in the Sacramento–San Joaquin Delta under climate-change scenarios and ecological implications. Estuaries Coasts. [accessed 2024 Sep 24];34:544–556. *https://doi.org/10.1007/s12237-010-9369-z*

Whitley SN, Bollens SM. 2014. Fish assemblages across a vegetation gradient in a restoring tidal freshwater wetland: diets and potential for resource competition. Environ Biol Fish. [accessed 2024 Sep 24];97:659–674. *https://doi.org/10.1007/s10641-013-0168-9*

Whipple AA, Grossinger RM, Rankin D, Stanford B, Askevold RA. 2012. Sacramento–San Joaquin Delta historical ecology investigation: exploring pattern and process. A report of SFEIASCs Historical Ecology Program. Richmond (CA): San Francisco Estuary Institute–Aquatic Science Center. [accessed 2024 Sep 24]. 408 p. Available from: *https://www.noaa.gov/sites/default/files/legacy/document/2020/Oct/07354626278-1.pdf*

Windham–Myers L, Oikawa PY, Deverel SJ, Chapple D, Drexler JZ, Stern D. 2023. Carbon sequestration and subsidence reversal in the Sacramento–San Joaquin Delta and Suisun Bay: management opportunities for climate mitigation and adaptation. San Franc Estuary Watershed Sci. [accessed 2024 Sep 24];20(4). *https://doi.org/10.15447/sfews.2023v20iss4art7*